Universidade de Aveiro Departamento de Química
2014

João Henrique Picado Madalena Santos

Estudo de novos processos downstream com base em métodos de FPLC e SAB

Designing new downstream processes based in FPLC and ABS methodologies

Universidade de Aveiro Departamento de Química
2014

João Henrique Picado Madalena Santos

Estudo de novos processos downstream com base em métodos de FPLC e SAB

Designing new downstream processes based in FPLC and ABS methodologies

Dissertação apresentada à Universidade de Aveiro para cumprimento dos requisitos necessários à obtenção do grau de Mestre em Biotecnologia, ramo de Biotecnologia Industrial e Ambiental, realizada sob a orientação científica do Professor Dr. Adalberto Pessoa-Junior, Professor Titular da Faculdade de Ciências Farmacêuticas) da Universidade de São Paulo e co-orientação da Dra. Sónia Patrícia Marques Ventura, Estagiária de Pós – Doutoramento da Universidade de Aveiro

A ti **Avó Dina**, que me deixaste mal acostumado. Foste, és e serás sempre o meu pilar.

o júri
Presidente

Prof. Dr. João Manuel da Costa Araújo Pereira Coutinho

professor catedrático do Departamento de Química da Universidade de Aveiro

Doutora Ana Paula Moura Tavares

investigadora do LSRE da Faculdade de Engenharia da Universidade do Porto

Doutora Sónia Patrícia Marques Ventura

estagiária de Pós-Doutoramento do Departamento de Química da Universidade de Aveiro

Agradecimentos

Em primeiro lugar gostaria de agradecer ao Prof. João Coutinho, ao Prof. Adalberto Júnior e à Dra. Sónia Ventura pela enriquecedora oportunidade que me proporcionaram de realizar Intercâmbio na conceituada Universidade de São Paulo. Sem o vosso voto de confiança este sonho nunca se teria realizado.

Um muito obrigado aos meus orientadores, Dra. Sónia Ventura e Prof. Adalberto pela amizade e apoio que deram, estando sempre disponíveis e prontos a ajudar e esclarecer diversas dúvidas que foram surgindo ao longo do percurso.

Aos meus pais, Henrique e Ana, e irmã pelo carinho e força que me deram, principalmente quando estava longe de casa e as saudades apertavam. Amplio este obrigado à minha madrinha, Rosa, aos meus tios, primos e avós que sempre estiveram do meu lado. Incluindo a Lina, minha tia brasileira.
Obrigado a todos os membros do Laboratório de Biotecnologia Farmacêutica, em especial ao Grupo Asparaginase (André, Karin, Juan Carlos, Johanna, Laura e Albert), ao João Molino pelo auxílio no FPLC, às simpáticas Rafinha, Bruna e Suellen pelos sorrisos, à Lina e ao Iván pela amizade e ao César e Ignácio por me fazerem companhia no laboratório em horas tardias, bem como os ensinamentos na língua espanhola. Obrigado também a Sarah pela ajuda na área da Toxicologia e à Prof. Maria Aurora Prado e às colegas Laura e Aline pela ajuda no manuseamento no equipamento de electroforese capilar.

Aos colegas de casa da Rua Otávio Passos nº.3, à família Santana que me fez sentir em casa, ao Júnior e Andreza por toda a hospitalidade e amizade, à Renata e sua família linda que sempre se interessaram por meu trabalho. Obrigado também aos amigos de Ílhavo que foram essenciais nesta aventura, em especial à Steph, Kiki, Catarina, Inês e Sofia. Um muito especial obrigado a ti, Ana Pedro, pelo teu carinho e apoio dado pelas chamadas de Skype. Aos amigos da faculdade: à Sílvia, Andreia, Pedro, Maria João, Ricardo, Deisy, Couceiro, Marli, Inês, Renata, Patrícia e tantos outros.

Quero também agradecer a todos os membros do grupo PATh por toda amizade e auxílio dado desde o primeiro momento que entrei neste laboratório. Em especial à Chica pela tamanha paciência que teve e tem comigo, à Tânia, ao Jorge, ao Kiki e à Ana Filipa por estarem sempre disponíveis a esclarecer dúvidas e inevitavelmente à Sara, ao Emanuel e à Luísa que foram três grandes amigos e colegas de laboratório.

Por fim, agradeço a todos os familiares e amigos que não mencionei, que fizeram parte desta experiência inesquecível, que me fez crescer como pessoa e investigador. A vocês um grande abraço e estou certo que vão continuar presentes na minha vida e no meu coração.

palavras-chave

Processos downstream, sistemas aquosos bifásicos, cromatografia de afinidade, FPLC, líquidos iónicos, eletrólitos, L-Asparginase I

Resumo

O objetivo principal deste trabalho foi a concepção de novos processos *downstream* para aplicações analíticas e biotecnológicas. Este trabalho foi dividido em três partes principais: formulação de novos SAB formados por polímeros, dependentes do uso inovador de líquidos iónicos como eletrólitos; design de sistemas aquosos bifásicos como uma alternativa para a extração da benzoilecgnonina e dois alucinógenos (harmina e harmalina); purificação por FPLC da L – Asparaginase I. Para cada capítulo, um resumo mais detalhado foi elaborado. Mostra-se que os bioprocessos de separação aqui estudados nomeadamente SAB e FPLC são alternativas viáveis às demais, devido aos altos rendimentos e maior seletividade obtidos. Para além disso, estes são relativamente simples e rápidos e de um ponto de vista operacional, apresentam baixo custo e são fáceis de escalonar.

A partir dos estudos analíticos, concluiu-se que mais trabalhos são necessários para a aplicação de SABs como plataformas de extracção de drogas ilícitas, principalmente por causa da baixa concentração das mesmas em matrizes complexas, como a urina e *Ayahuasca*. Melhores resultados foram obtidos, quando se utilizou os SABs como plataformas de extracção de compostos biotecnológicos, em que foi possível maximizar o desempenho de extracção tanto do citocromo c como do ácido cloranílico, utilizando baixas concentrações de líquido iónico (0,1 % em massa), como eletrólitos. Também a purificação por FPLC da His-Tagg ASPase I recombinante foi efectuada com sucesso, obtendo uma recuperação de 81,03 ± 0,01 % e um fator de purificação 17 vezes relativamente à amostra original, proveniente do meio fermentativo.

Keywords

Downstream processes, aqueous biphasic systems, affinity chromatography, FPLC, ionic liquids, electrolytes, L- Asparaginase I.

Abstract

The main objective of this work was the design of novel downstream processes for analytical and biotechnological applications. This work was divided in three major topics: formulation of novel polymer-based ABS systems with innovative use of IL as electrolytes; design of aqueous biphasic systems as an alternative for extraction of benzoylecgnonine and two hallucinogens (harmine and harmaline); FPLC purification of L-Asparaginase I. For each chapter, a detailed summary is presented. The downstream processes herein studied namely ABS and FPLC are good alternatives, due to the high yields and enhanced selectivity obtained. Moreover, they are relatively simple and fast from the operational point of view, present a low cost and are easy to scale up.

The analytical studies show that further work is required for the application of ABS as drug extracting platforms, mainly because of the very low concentration of drugs in complex matrixes, such as urine and *Ayahuasca*. Better results were obtained using ABS as biotechnological extracting platforms, being possible to maximize the extractive performance of Cyt c and CA, using low concentrations of IL (0.1 wt%) as electrolytes. Furthermore, the FPLC purification of His-Tagg recombinant ASPase I was successfully performed, obtaining a recovery of 81.03 ± 0.01 % and a purification factor of 17 times relatively to the original sample from fermentation broth.

Contents

List of tables

List of figures

[C_2mim][Tos] (+), [C_2mim][CF_3SO_3] (◆) + K_3PO_4 at (298 ± 1) K. Binodal curves adjusted using Eq.5 are represented in dashed lines. The influence of IL's structural features is provided separately in the insets to simplify the analysis.

Figure 15. Liquid chromatogram of benzoylecgonine standard (100 ppm).

Figure 16. HPLC chromatogram of the benzoylecgonine standard (black line), of the IL-rich phase of blank human urine-based ABS (blue line) and of the IL-rich phase of drug-containing human urine-based ABS (violet line).

Figure 17. HPLC chromatogram of the benzoylecgonine standard (black line), of the salt-rich phase of blank human urine-based ABS (blue line) and of the salt-rich phase of drug-containing human urine-based ABS (violet line).

Figure 18. Electropherogram of harmine and harmaline (100 ppm). Conditions: MEKC buffer containing 20 mM sodium tetraborate, TBS (pH 9.40), 40 mM SDS, 10 % (v/v) methanol. Capillary 20 cm to the detector and 50 μm i.d., Applied current: 70 μA, hydrodynamic injection 0.5 psi for 30 seconds, T = (293.1 ± 0.1) K, at a wavelength of 336 nm.

Figure 19. (a) [C_2mim]Cl/K_3PO_4-based ABS extraction of hallucinogens from *Ayahuasca* pre-treated sample, in which [C_2mim]Cl and K_3PO_4 are the top and bottom phase respectively. (b) PEG 8000/NaPA 8000-based ABS extraction of hallucinogens from *Ayahuasca* pre-treated sample, in which PEG and NaPA are the top and bottom phase respectively.

Figure 20. Electropherogram of IL-rich phase of [C_2mim]Cl/K_3PO_4-based ABS prepared using the *Ayahuasca* pre-treated sample. Conditions: MEKC buffer containing 20 mM sodium tetraborate, TBS (pH 9.40), 40 mM SDS, 10 %(v/v) methanol. Capillary 20 cm to the detector and 50μm i.d. , Applied current: 70 μA, hydrodynamic injection 0.5 psi for 30 seconds, T = (293.1 ± 0.1)K, wavelength 336 nm.

Figure 21. Electropherogram of salt-rich phase of [C_2mim]Cl/K_3PO_4-based ABS prepared using the *Ayahuasca* pre-treated sample. Conditions: MEKC buffer containing 20 mM sodium tetraborate, TBS (pH 9.40), 40 mM SDS, 10 %(v/v) methanol. Capillary 20 cm to the detector and 50μm i.d. , Applied current: 70 μA, hydrodynamic injection 0.5 psi for 30 seconds, T = (293.1 ± 0.1)K, wavelength 336 nm.

Figure 22. Electropherogram of PEG 8000-rich phase of PEG 8000/NaPA 8000-based ABS with [C_2mim]Cl as electrolyte prepared using the *Ayahuasca* pre-treated sample. Conditions: MEKC buffer containing 20 mM sodium tetraborate, TBS (pH 9.40), 40 mM SDS, 10 %(v/v) methanol. Capillary 20 cm to the detector and 50μm i.d. , Applied current: 70 μA, hydrodynamic injection 0.5 psi for 30 seconds, T = (293.1 ± 0.1)K, wavelength 336 nm.

Figure 23. Electropherogram of NaPA 8000-rich phase of PEG 8000/NaPA 8000-based ABS with [C_2mim]Cl as electrolyte prepared using the *Ayahuasca* pre-treated sample.

Conditions: MEKC buffer containing 20 mM sodium tetraborate, TBS (pH 9.40), 40 mM SDS, 10 %(v/v) methanol. Capillary 20 cm to the detector and 50μm i.d. , Applied current: 70 μA, hydrodynamic injection 0.5 psi for 30 seconds, T = (293.1 ± 0.1)K, wavelength 336 nm.

Figure 24. Overview of normal human hematopoiesis[109]. Blood or Hematopoietic stem cells (HSCs) give rise to the myeloid (monocytes and macrophages, neutrophils, basophils, eosinophils, erythrocytes, megakaryocytes/platelets, dendritic cells), and lymphoid lineages (T-cells, B-cells, NK-cells).

Figure 25. Schematic representation of the crystal L-asparaginase, resolution of 1.82 Å. (Extracted from Protein Data Bank, PDB code 2HIM).

Figure 26. (a) FPLC™ (System ÄKTApurifier) formed by Pump P-900, Monitor UV-900, Monitor UPC-900, Valve INV-907, Mixer M-925 and Valves SV-903, FV-923 (b) HiTrap™ 5 mL IMAC FF column

Figure 27. Linear gradient of imidazole used in FPLC purification, obtained from FPLC software. The blue line corresponds to absorbance at 280 nm. The black boxes (fractions 14-18 and 20-31)

Figure 28. Polyacrylamide gel electrophoresis combined with silver staining, showing the purified samples from linear step FPLC purification. The black boxes highlight the wash-out unbound proteins (second lane) and histidine-tagged ASNase I bands (~ 45.0 KDa). In the different lanes are represented the eluted fractions and PM refers to Protein Markers.

Figure 29. Polyacrylamide gel electrophoresis combined with silver staining, showing the purified samples from two-step FPLC purification. The brown box highlights the his-tagged ASNase I bands (~ 45.0 KDa). In the different lanes are represented the eluted fractions and PM refers to Protein Markers.

List of Symbols

EA – Enzymatic activity (in $IU.mL^{-1}$)

EE_{CA} – Extraction efficiency of chloranilic acid (in %)

$EE_{Cyt\ c}$ - Extraction efficiency of cytochrome c (in %)

i.d. – Internal diameter (in μm)

K_{CA} - Partition coefficient of chloranilic acid

K_{IL} - Partition coefficient of ionic liquid

PF – Purification factor

RT – Retention time (in min)

SA – Specific enzymatic activity (in $IU.mg^{-1}$)

T – Temperature (in K)

List of abbreviations

ABS – Aqueous biphasic system

ALL - Acute lymphoblastic leukemia

ASNase – L-Asparaginase

Asn - Asparagine

ASP1 – Asparaginase I (gene)

BE – Benzoylecgonine

CA – Chloranic acid

Cyt c – Cytochrome c

CE – Capillary electrophoresis

FPLC - Fast Protein Liquid Chromatography

IL(s) – Ionic liquid(s)

IU – International unit of enzyme activity

MEKC - Micellar Electrokinetic Chromatography

[C_2mim]Cl - 1-ethyl-3-methylimidazolium chloride

[C_2mim][DMP] - 1-ethyl-3-methylimidazolium dimethylphosphate

[C_2mim][CH_3SO_3] - 1-ethyl-3-methylimidazolium methanesulfonate

[C_2mim][Tos] - 1-ethyl-3-methylimidazolium tosylate

[C_2mim][CH_3CO_2] - 1-ethyl-3-methylimidazolium acetate

[C_2mim][CF_3SO_3] - 1-ethyl-3-methylimidazolium triflate

[C_2mim][$N(CN)_2$] - 1-ethyl-3-methylimidazolium dicyanamide

[OHC_2mim]Cl - 1-(2-hydroxyethyl)-3-methylimidazolium chloride

[$N_{2,2,2,2}$]Cl - tetraethylammonium chloride

[$N_{2,2,2,2}$]Br - tetraethylammonium bromide

[C_{14}mim]Cl - 1-tetradecyl-3-methylimidazolium chloride

[Ch]Cl - choline chloride

NaCl - Sodium chloride

Na_2SO_4 - Sodium sulphate

General Context

Biological compounds are important for many applications including bio-transformations, diagnostics, research and development, food processes, pharmaceutical products, and toxicological studies. Depending of their usage, biological products can be obtained from crude extracts, fermentation broth, industrial wastes or biological raw materials (micro and macroalgae), with any previous purification and consequently exhibiting high contaminant content. For toxicological analysis, these products, that may or may not be biological (*e.g.* synthetic drugs) are required to be extracted from complex matrixes (*e.g.* hair, urine or blood). Nevertheless, some bioproducts, such as biopharmaceuticals typically require exceptional purity, making downstream processing the critical step of the overall process[1]. The downstream stage in industrial biotechnology refers to recovery, purification and isolation, of the microbial products from cell debris, processing medium and contaminant biomolecules from the upstream process into a finished product such as enzymes, dyes and proteins[1,2]. The downstream process design has the greatest impact on the overall bio-manufacturing costs because, not only does the biochemistry of different products (e.g., peptides, proteins, hormones, antibiotics, and complex antigens) dictate different methods for the isolation and purification of these products but also, the contaminating by-products can reduce the overall process yield, and may have serious consequences on clinical safety and efficacy. Therefore, downstream separation scientists and engineers are continually seeking to eliminate or combine unit operations to minimize the number of process steps, in order to maximize the product recovery at a specified concentration and more important, with a specific and very high purity level[3,4].

The downstream processes are continuously facing diverse challenges, namely considering the *Biological products which are often present in very low concentration* (e.g. monoclonal antibodies concentration of 0.1 $mg.mL^{-1}$ in the mammalian cell culture supernatants). Therefore, in many cases, large volumes of dilute product streams have to be processed. For toxicological analysis, the toxins/drugs concentration is in an even lower concentration (in the order $ng.mL^{-1}$); *many impurities and by-products are present in the source material and they have chemical and physical properties similar to those of the*

target product, which makes separation processes extremely challenging. Hence, bioseparation has to combine high yields and high selective to insure the product stability; *there are stringent quality requirements for products used for pharmaceutical, diagnostic and therapeutic purposes*, both in terms of active product content as well as in terms of the absence of specific impurities (e.g. injectable therapeutic products should be free from endotoxins and pyrogens). The design of these downstream processes is more problematic, due to the demanding purification requirements. Generally there is a need of a higher number of purification steps, reflected in a higher cost of overall downstream process; *Biological products are susceptible to denaturation and other forms of degradation*. Therefore bioseparation techniques have to be "gentle" in terms of avoiding extremes of physicochemical conditions such as pH and ionic strengths, hydrodynamic conditions such as high shear rates, and exposure to gas-liquid interfaces. Organic solvents which are widely used in chemical separations have relatively limited usage in bioseparations on account of their tendency to promote degradation of many biological products; *many biological products are thermolabile* and hence many bioseparation techniques are usually carried out at sub-ambient temperatures; *bioseparation is frequently based on multi-technique separation*, where different downstream processes are interlinked in order to have an enhanced purification[4–7]. A widely recognized heuristic, also known as RIPP (Recovery, Isolation, Purification and Polishing) is commonly used in bioseparation[8]. This scheme categorizes downstream processing operations dividing them into four groups, which are applied in order to bring a product from its source as a component of a tissue, cell or fermentation broth, through progressive improvements in purity and concentration:

1. *Clarification or removal of non-soluble* is the first step and it involves the capture of the product as a solute in a particulate-free liquid, for example the separation of cells, cell debris or other particulate matter from fermentation broth containing an antibiotic. Typical operations to achieve this are filtration, centrifugation, sedimentation, precipitation, flocculation, electro-precipitation, and gravity settling. Additional operations such as grinding, homogenization, or leaching are required to recover products from solid sources, such as plant and animal tissues, are also usually included in this group[9].

2. *Product isolation* is the removal of those components whose properties vary markedly from that of the desired product. For most products, water is the chief impurity and isolation steps are designed to remove most of it, reducing the volume of material to be

handled and concentrating the product. Solvent extraction, adsorption, ultrafiltration, and precipitation are some of the unit operations involved[4,6].

3. *Product purification* is done to separate those contaminants that resemble the product very closely in physical and chemical properties. Consequently, steps in this stage are expensive to carry out and require sensitive and sophisticated equipment. This stage contributes to a significant fraction of the entire downstream processing expenditure. Examples of operations include affinity, size exclusion, reversed phase chromatography[2], crystallization[4], fractional precipitation[8] or liquid-liquid extraction[10].

4. *Product polishing* describes the final processing steps which end with packaging of the product in a form that is stable, easily transportable and convenient. Crystallization, desiccation, lyophilisation and spray drying are typical unit operations[7]. Depending on the product and its intended use, polishing may also include operations to sterilize the product and remove or deactivate trace contaminants which might compromise product safety. Such operations might include the removal of viruses or depyrogenation.

The high-throughput, low-resolution techniques are first used to significantly reduce the volume and overall concentration of the material being processed. In the other hand, the partially purified products are then further processed by high-resolution low-throughput techniques to obtain pure and polished finished products[3,8].

General objectives

In this work we pretended to design novel extraction techniques to be applied as downstream processes based in FPLC and ABS methodologies.

It is our intention to create new polymer-based ABS, with the innovative addition of ionic liquids as electrolytes to overcome the limited range of polarities of the phase polymers and consequently promote the phase separation. Moreover, the influence of several parameters on the ABS formation, namely the ILs' presence, structural features (in particular IL family and anion conjugated) and concentration were study. We intend to find the smallest IL concentration that exhibit high extraction efficiency. Extraction studies with probe molecules, in particular, chloranilic acid and cytochrome c were accomplish in order to discern the yield and extraction efficiency of these systems as extraction platforms (Chapter I).

Then, and after the proper design of these polymeric ABS, it is proposed the design of aqueous biphasic systems as an alternative for extraction of benzoylecgnonine and two hallucinogen compounds, namely harmine and harmaline from complex matrixes, respectively human urine and *Ayahuasca*. The analytical method was based on two stages: the first consists on the sample pre-concentration using ionic liquids-based aqueous biphasic systems (namely ILs as electrolyte and IL/salt systems); the second involves the quantification of the target compounds by HPLC for benzoylecgonine and capillary electrophoresis for both hallucinogens (Chapter II).

Finally it was intended to purify L-ASNase I with a low number of purifying steps, obtaining a pure enzyme with high yields and specific activity, using FPLC downstream process, in order to be scaled-up for a promissory commercial pharmaceutical application. The FPLC purification was performed in two different stages. In the first stage a linear gradient, running from 0 mM to 500 mM of imidazole at 5.0 $mL.min^{-1}$ was perform in order to identify the lowest imidazole concentration of the elution buffer that extracts the higher amount of L-ASNase I. In the second stage, two-step gradient of imidazole was performed for an optimized L-ASNase I purification. Polyacrylamide gel electrophoresis combined with silver staining and Nessler activity assay were also used in order to confirm the presence of the purified L-Asparaginase I (Chapter III).

Chapter I

Ionic liquids as a novel class of electrolytes in polymeric aqueous biphasic systems

Abstract

The design of a novel eco-friendly and cheap aqueous biphasic systems composed of two polymers, namely poly(ethylene glycol) of average molecular weight 8000 $g.mol^{-1}$ and sodium poly(acrylate) of molecular weight 8000 $g.mol^{-1}$ (here designed by PEG 8000 and NaPA 8000) using ionic liquids (ILs) as electrolytes and their application in (bio)separation processes are here attempted. The binodal curves were established at (298 ± 1) K and atmospheric pressure, considering distinct ILs and inorganic salts. These systems enabled the assessment of the influence of several parameters on the ABS formation, namely the ILs' presence, structural features (in particular IL family and anion conjugated) and concentration. In general, ILs revealed the capability to act as electrolytes, promoting the phase separation. Moreover, the resulting ABS were characterized in terms of the ILs partitioning behaviour, which preferentially occurred towards the NaPA 8000-rich phase, and the media pH. The capacity of these ABS in terms of extraction technologies was tested taking into account the goal of carrying out partition experiments for two distinct molecules, namely the protein cytochrome c (Cyt c) and the probe dye chloranilic acid (CA). The results suggest that they displayed opposite migrations: Cyt c was totally recovered in the NaPA 8000-rich phase ($EE_{Cyt\ c}$ > 96.13 ± 3.22 % when ILs are present acting as electrolytes), while CA is selectively migrating towards the PEG 8000-rich phase (EE_{CA} > 80.13 ± 1.45 % for IL as electrolytes). The decrease of the IL concentration on the polymer-based ABS leads to a significant increase in the partition coefficient of CA (K_{CA}) towards the PEG 8000-rich phase, suggesting that the use of low amounts of IL (0.1 wt%, for example) is an advantageous condition to boost the extractive performance of different bio(molecules) including Cyt c and CA.

1.1. Introduction

Aqueous biphasic systems (ABS) were originally proposed by Albertsson[11] as cleaner liquid-liquid extraction processes that could be used as potential substitutes for the conventional ones. This is mainly due to the fact that ABS are not derived from hazardous and volatile organic solvents and present abundant water contents[12], providing milder and more biocompatible conditions for bioseparation/downstream processes. In fact, ABS are able to maintain the native conformation and biological activity of diverse biomolecules, while exhibiting high yields and purity levels. Evidences of their successful application are well-documented for a wide array of compounds, namely proteins[8,13–15], enzymes[16,17], cells[18,19] and antibiotics[20–22]. Apart from their environmentally benign status, ABS are full of flexibility related with the countless types of chemical compounds that can be combined to create them, *e.g.* polymer + polymer[15,17,23,24], polymer + salt[20,25,26] or salt + salt[27–30].

Polyethylene glycol (PEG) is a non-ionic polymer commonly used in the ABS domain, since it presents advantageous characteristics in terms of biodegradability, toxicity and cost-effectiveness. In order to create polymeric ABS, blends of PEG with other polymers, such as maltodextrin[23,24] and specially dextran[13,31], are within the most common options. However, these are expensive and display high viscosities and opacities as well as limited range of polarities of the phases. Moreover, although the number of polymers is huge, some of the potential polymer pairs are not able to form ABS, limiting the variety of systems. This scenario triggered the creation of novel lines of research focused on the search for improved ABS capable of overcoming such drawbacks.

One of the proposed strategies regards the minimization of the polymers' amounts, *i.e.* increasing those of water. This can be attained through the complementary addition of small amounts of salts (*e.g.* 1.05 to 6 wt%)[32] acting as electrolytes and allowing the phase split. In systems without salt addition the two-phase formation only occurs at very high polymer concentrations, and therefore, the presence of these salts is mandatory for the ABS formation. For instance, NaCl (sodium chloride), Na_2SO_4 (sodium suflate), NaOOC-$(CH_2)_7$-COONa (di-sodium azelate) and NaOOC-$(CH_2)_4$-COONa (di-sodium adipate) have been successfully applied as electrolytes in polymeric ABS composed of PEG-sodium polyacrylate (NaPA)[32] and PEG-poly(acrylic) acid (PA)[33,34]. At the end, properly selecting the electrolyte structure, it was possible to increase the biphasic region[32], making possible to work at very low polymer concentrations (*e.g.* 10 wt% of each polymer). Indeed, these

systems have been widely applied to the extraction of proteins, namely, hemoglobin[15], lysozyme[15], glucose-6-phospate dehydrogenase (G6PDH)[15] and green fluorescent protein (GFP)[14]. Since such systems were shown to maintain the native conformation and biological activity of biomolecules, associated with high yields of purification[14,15], they are believed to be more biocompatible routes. Another approach passed for the substitution of one of the polymers by a high melting temperature salt which benefits from somehow lower viscosities and opacities of the whole ABS. More recently, the use of ionic liquids (ILs) as either main phase forming agents[35–37] or adjuvants[38–40] (addition of small amounts of ILs, *at circa* 5 wt%) emerged. Remarkably, the introduction of such ionic compounds in polymeric ABS significantly enlarges the polarity differences between the phases[35,40]. ILs are salts in the liquid state below a stated temperature of 100 ºC, conventionally composed of a large organic cation and an anion of either inorganic or organic nature[28]. They present unique characteristics such as, the insignificant vapour pressure and flammability, being these the main reasons why ILs are labelled as *greener solvents*. Moreover, they possess high chemical and thermal stabilities[28] and outstanding capability of solvating compounds from a wide spectrum of polarities[35,41]. These characteristics have contributed for the recognition of ILs as fascinating phase forming agents in ABS. Furthermore, the ILs' status of *designer solvents*[42], *i.e.* (almost) immeasurable cation/anion possible combinations, brings the possibility to manipulate ABS phases' polarities and to develop systems with affinities for certain tailored application.

In this work, ILs were applied as electrolytes in the domain of polymeric ABS. The experimental phase diagrams of ABS based on polyethylene glycol (PEG) and sodium polyacrylate (NaPA), both with the same molecular weight of 8000 $g.mol^{-1}$, were established at (298 ± 1) K and atmospheric pressure. The choice of these polymers was supported by their simple recycling that enables their application at larger scale[32]. Different imidazolium and ammonium-based ILs and two high melting temperature salts, NaCl and Na_2SO_4, were applied as electrolytes. These allowed the comparative assessment between the performance of ILs and inorganic salts as electrolytes in polymeric ABS. Testing out the *designer solvent* status, it was possible to investigate the impact of several structural modifications at the level of the cation core and the anion moiety on the binodal curves behaviour. Moreover, these novel ABS were characterized in terms of electrolyte (imidazolium-based ILs) partition between the phases and pH of the aqueous medium. The

ABS here developed were then applied in the extraction of two different molecules, the Cytochrome c (Cyt c) and Chloranilic acid (CA), herein used as model compounds. Cyt c is an electron-carrying mitochondrial heme protein (red colour) containing a single polypeptide chain and a single heme group, which is covalently attached to cysteine residues, namely: Cys-14 and Cys-17. The ready fluctuation of Cyt c within the cell between the ferrous and ferric states makes it an efficient biological electron-transporter, which plays a vital role in cellular oxidations in both plants and animals. It is generally regarded as a universal catalyst of respiration, forming an essential electron-bridge between the respirable substrates and oxygen[43]. CA is a small organic dye presenting red-brown colour in dry conditions or violet in aqueous medium[35]. The main field of application of CA is in the analytical chemistry, for spectrophotometric determinations (*e.g.* determination of three macrolides *i.e.*, erythromycin, roxithromycin and clarithromycin through charge transfer complexes[44]). These molecules were considered as probe molecules, due to their very distinct chemical structure and complexity, and their activity. The extractive performance of these systems was investigated by using the imidazolium-based ILs at distinct concentrations, and the inorganic salts (for comparative analysis).

1.2. Materials and methods

1.2.1. Materials

PEG 8000 and the aqueous solution of NaPA 8000 (45 wt%) were purchased at Sigma-Aldrich® and were used as received. The salts $NaSO_4$ and NaCl were acquired at Synth®. The two molecules CA (purity > 99 wt%) and Cyt c from equine heart (purity = 95 wt%) were purchased at Merck® and Sigma-Aldrich®, respectively. Their chemical structures are provided in Figure 1. Eleven distinct ILs were used: 1-ethyl-3-methylimidazolium chloride $[C_2mim]Cl$ (purity > 98 wt%), 1-ethyl-3-methylimidazolium dimethylphosphate $[C_2mim][DMP]$ (purity > 98 wt%), 1-ethyl-3-methylimidazolium methanesulfonate $[C_2mim][CH_3SO_3]$ (purity > 99 wt%), 1-ethyl-3-methylimidazolium tosylate $[C_2mim][Tos]$ (purity = 99 wt%), 1-ethyl-3-methylimidazolium acetate $[C_2mim][CH_3CO_2]$ (purity > 95 wt%), 1-ethyl-3-methylimidazolium triflate $[C_2mim][CF_3SO_3]$ (purity = 99 wt%), 1-ethyl-3-methylimidazolium dicyanamide $[C_2mim][N(CN)_2]$ (purity > 98 wt%), 1-(2-hydroxyethyl)-3-methylimidazolium chloride $[OHC_2mim]$ Cl (purity = 99 wt%), tetraethylammonium chloride $[N_{2,2,2,2}]Cl$ (purity > 98%), tetraethylammonium bromide $[N_{2,2,2,2}]Br$ (purity > 98 wt%) and choline chloride [Ch]Cl (purity > 98 wt%). The imidazolium based-ILs were acquired at Iolitec® (Ionic Liquid Technologies, Germany). $[N_{2,2,2,2}]Cl$ and [Ch]Cl were acquired from Sigma-Aldrich®, while $[N_{2,2,2,2}]Br$ was purchased at Fluka AG – Chemische. The $[C_{14}mim]Cl$ studies are presented in *1.5. Future work* section. The chemical structures of all ILs are depicted in Figure 2. The water used was double distilled, passed by a reverse osmosis system and further treated with a Milli-Q plus 185 water purification apparatus.

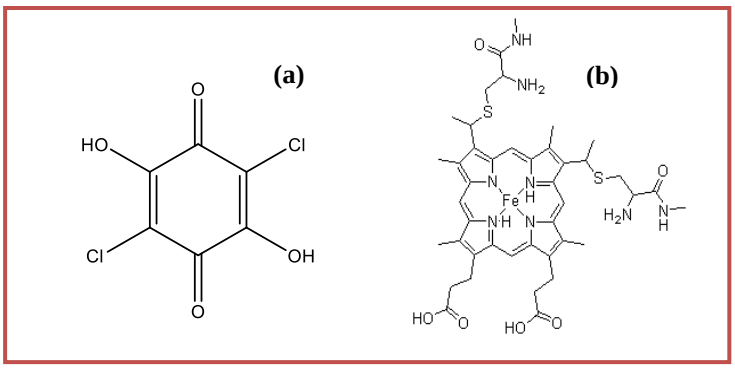

Figure 1. Chemical structure of CA (a) and horse heart Cyt c (b).

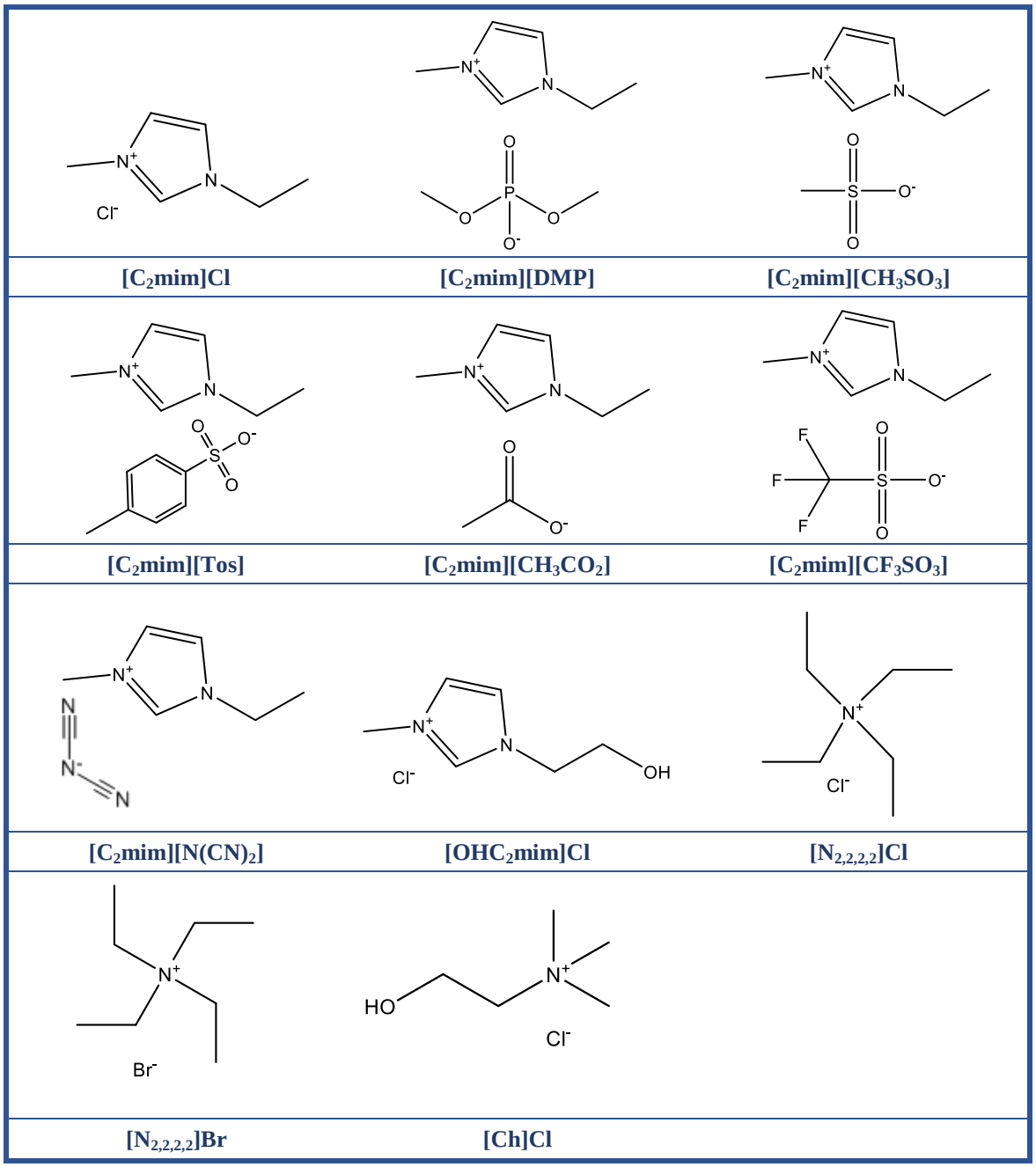

Figure 2. Chemical structure and abbreviations of the ILs studied in this work.

1.2.2. Binodal curves determination

The experimental binodal curves were determined using the cloud point titration method at (298 ± 1) K and atmospheric pressure, following a protocol previously described in literature[45]. Briefly, three stock aqueous solutions were prepared: 50 wt% of PEG 8000 + 5 wt% of IL or inorganic salt, 40 wt% of NaPA 8000 + 5 wt% of IL or inorganic salt and water + 5 wt% of IL or inorganic salt. Additionally, the IL/inorganic salt concentration was varied from 5 wt% to 2.5 wt% and 0.1 wt%, aiming to assess its effect on the behaviour of

the binodal data. Drop-wise addition of a PEG 8000-containing solution was performed to a solution of NaPA 8000 until the visual detection of two phases. Subsequently, drop-wise addition of the IL/inorganic salt-containing solution was conducted until the two phases disappear (monophasic region). This procedure was repeated several times to obtain the binodal curve, being performed under constant stirring, within an uncertainty of ± 10^{-4} g. The experimental phase diagrams data were correlated using the Merchuk equation[46] (1), described as follows:

$$[PEG\ 8000] = A \exp[(B \times [NaPA\ 8000]^{0.5}) - (C \times [NaPA\ 8000]^{3}) \qquad \textbf{(1)}$$

where [PEG 8000] and [NaPA 8000] represent the weight percentages of PEG 8000 and NaPA 8000, respectively and *A*, *B* and *C* are constants obtained by the regression of the experimental data. The Merchuk equation was chosen since it has a low number of adjustable parameters to correlate these data and it is the most commonly used[30].

1.2.3. Partitioning studies of Cyt c, CA and ILs

A mixture point within the biphasic region was selected and prepared by weighing the appropriate amounts of each compound: 15 wt% of PEG 8000 + 4.5 wt% of NaPA 8000 + 5 wt% of electrolyte + 0.1 g of a Cyt c stock solution (*at circa* 5.0 g.L^{-1}) or 1 g of a CA stock solution (*at circa* 0.72 g.L^{-1}) for 5 g of total mass. For the partitioning studies of the target molecules, only the imidazolium-based ILs and the inorganic salts were used. To investigate the effect of electrolyte concentration, systems containing $[C_2mim][N(CN)_2]$ and NaCl were selected to carry out partitioning studies of CA. The same mixture compositions aforementioned were prepared, varying only the amount of electrolyte from 5 wt% to 2.5 wt% and 0.1 wt%. All the components were mixed together using a Vortex agitator (IKA, C-MAG HS7), and then equilibrated at (298 ± 1) K and atmospheric pressure during 12 h, allowing the equilibrium to be reached. At the end, the final systems resulted in two clear phases, a PEG 8000-rich as the top and a NaPA 8000-rich as the bottom layer, with a well-defined interface in between. The coexisting phases were then carefully separated and collected for the measurement of their volumes, weights and pH values as well as for the quantification assays.

The determination of the target compounds and imidazolium-based ILs content was assessed using a Molecular Devices Spectramax 384 Plus | UV-Vis Microplate Reader, at the respective maximum wavelength of absorbance, namely 409 nm for Cyt c, 330 nm for

CA, and 211 nm for all ILs (except the choline and ammonium structures). At least three independent samples of each system were prepared, being the average values reported along with the respective standard deviations.

The IL partition coefficient (K_{IL}) was calculated as the ratio between the amount of IL present in the bottom and top phases, as described by Eq. 2:

$$K_{IL} = \frac{Abs(IL_B)}{Abs(IL_T)} \quad \textbf{(2)}$$

where Abs*(*IL_B*)* and Abs*(*IL_T*)* are the IL absorbance output measured for the bottom and top phases, respectively.

The CA partition coefficient (K_{CA}) is defined by the ratio of the CA concentration in the top phase, $[CA]_T$, to that in bottom the phase, $[CA]_B$ – Eq. 3.

$$K_{CA} = \frac{[CA]_T}{[CA]_B} \quad \textbf{(3)}$$

The percentage extraction efficiency (EE, %) was calculated for both biomolecules following Eq. 4:

$$EE = \frac{V_{molecule-rich} \times [M]_{molecule-rich}}{V_i \times [M]_i} \times 100 \quad \textbf{(4)}$$

where V_i and $[M]_i$ are the initial volume and the initial concentration of molecule added to prepare the extraction systems, while $V_{molecule\text{-}rich}$ and $[M]_{molecule\text{-}rich}$ denote the volume and concentration of dye in the phase where it is more concentrated: top phase in the case of CA (EE_{CA}) and bottom phase for Cyt c ($EE_{Cyt\ c}$). It should be noted that blank controls where the CA or the Cyt c solutions were replaced by water were constantly applied to remove possible interferences from the phase components.

The pH values of both phases were measured at (298 ± 1) K using a Digimed DM-22 dual meter pH equipment with an uncertainty ± 0.02.

1.3. Results and discussion

1.3.1. Design of polymeric ABS with ILs as electrolytes

1.3.1.1. Electrolytes' impact on the ABS formation

Although Johansson *et al.*[32] have addressed the influence of inorganic salts as electrolytes in phase diagrams of ABS composed of PEG 2000, 4000 and 8000 and NaPA 8000, this is the first time that ILs have been used as electrolytes. The experimental binodal curves here determined and the respective adjustments by the Merchuk equation are provided in Figs. 3, 4 and 5 in molality units (mole of solute *per* kg of solvent), while the detailed experimental weight fraction data, respective correlations (adjusted parameters *A*, *B* and *C*) and binodal curves in mass fraction units are represented in Table A.1-6 and Fig. A.2-3 from Appendix A. The ILs employed allow the investigation of several parameters related with the application of ILs as electrolytes, namely the anion moiety, the cation core and their concentration. Table 1 reports all trends gauged for the electrolytes' aptitude to promote phase separation, organized according to each parameter evaluated.

The principal results demonstrate that, as for inorganic salts, NaCl and Na_2SO_4, ILs of different families are also capable to induce the formation of ABS (Fig. 3). Despite the higher capability of to induce the phase separation demonstrated by the inorganic salts, probably due to the higher charge density, it seems that the manipulation of the phase split can be achieved by adding distinct ILs by playing with the combination cation/anion (Fig. 3 and Table 1). However, it should be mentioned that these systems have in general higher capacity to induce the phase separation, when compared with other IL-containing ABS (*e.g.* IL + polymer, polymer + inorganic salt + IL as adjuvant, IL + salt)[28], as can be seen in Fig. 4, in Fig. B.3 from Appendix B the phase diagram is provided in mass fraction units. This is of major importance, since there is a natural interest to find out systems that can move the binodal curve closer to the water rich region in the phase diagram, due to the low component content (polymer/salt) required, reducing the overall cost and viscosity and increasing the biocompatibility of the ABS.

Table 1. General ranks of the electrolytes' aptitude to promote ABS formation.

Parameters	**Rank of the electrolytes' performance**
Salts *vs.* ILs	$NaCl \approx Na_2SO_4 > ILs$
IL anion moiety	$[C_2mim]$-based ILs: $[N(CN)_2]^- > [Tos]^- \approx [CF_3SO_3]^- > Cl^- > [CH_3CO_2]^- > [CH_3SO_3]^- > [DMP]^-$ $[N_{2,2,2,2}]$-based ILs: $Br^- > Cl^-$
IL cation core	Cl^--based ILs: $[Ch]^+ \approx [C_2mim]^+ > [OHC_2mim]^+ > [N_{2,2,2,2}]^+$
Electrolyte Concentration	NaCl: 5 wt% ≈ 2.5 wt% >> 0.1 wt% $[C_2mim][N(CN)_2]$: 5 wt% > 2.5 wt% >> 0.1 wt%

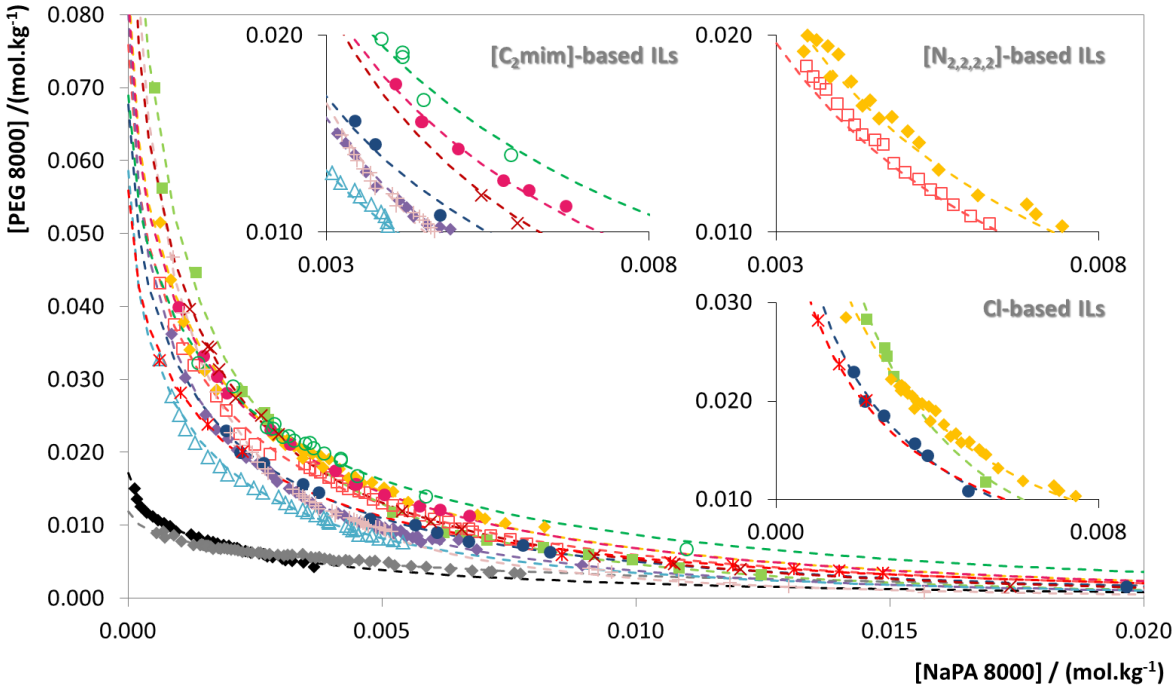

Figure 3. Binodal curves of the polymeric ABS containing 5 wt% of electrolyte (either inorganic salts or ILs): NaCl (◆), Na_2SO_4 (◆), $[C_2mim][N(CN)_2]$ (△), $[C_2mim][Tos]$ (+), $[C_2mim][CF_3SO_3]$ (◆), $[C_2mim]Cl$ (●), $[Ch]Cl$ (✳), $[OHC_2mim]Cl$ (■), $[C_2mim][CH_3CO_2]$ (×), $[N_{2,2,2,2}]Br$ (□), $[C_2mim][CH_3SO_3]$ (●), $[N_{2,2,2,2}]Cl$ (◆), $[C_2mim][DMP]$ (○). Binodal curves adjusted using Eq. 1 are represented in dashed lines. The influence of IL's structural features is provided separately in the insets to simplify the analysis.

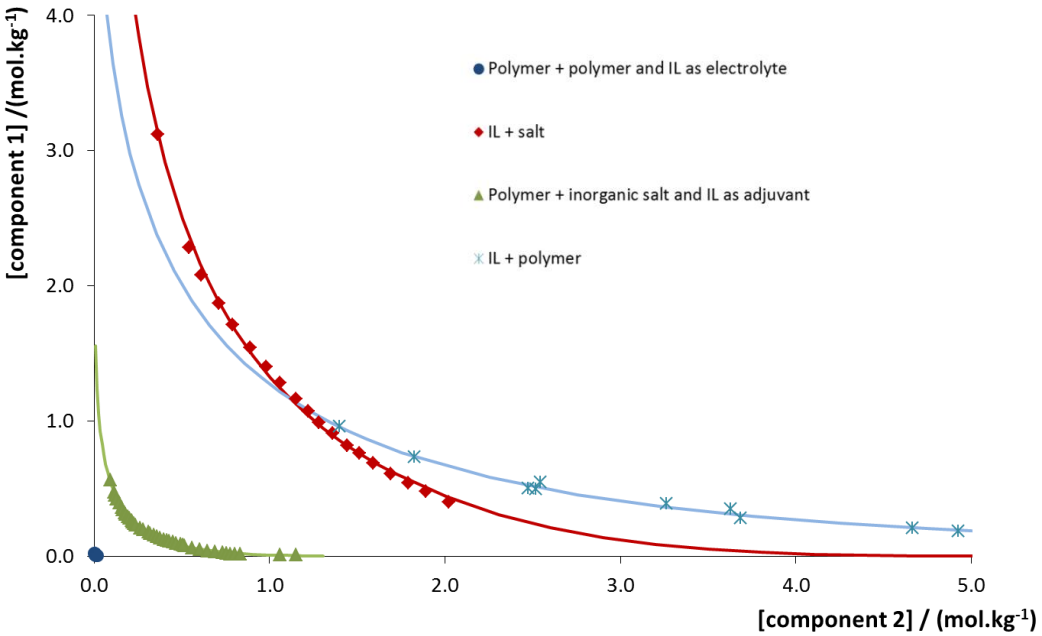

Figure 4. Binodal curves of different types of ABS: PEG 8000 (component 1) + NaPA 8000 (component 2) + $[C_2mim]Cl$ as electrolyte (●), $[C_2mim]Cl$ (component 1) + K_3PO_4 (component 2) (◆), PEG 1500 (component 1) + K_3PO_4 (component 2) + $[C_2mim]Cl$ as adjuvant (▲)[38], PEG 1500 (component 1) + $[C_2mim]Cl$ (component 2) (✳)[35].

The impact of several anion moieties on the polymeric ABS formation was assessed by using either $[C_2mim]$-based or $[N_{2,2,2,2}]$-based ILs and their binodal data are sketched in Fig. 3. Eight distinct anions, namely Cl^-, Br^-, $[DMP]^-$, $[CH_3SO_3]^-$, $[Tos]^-$, $[CH_3CO_2]^-$, $[CF_3SO_3]^-$ and $[N(CN)_2]^-$ were investigated, and their aptitude to promote the phase separation is given in Table 1. The trends here gauged are similar to those highlighted in previous works for ABS composed of imidazolium-[45] and ammonium-based[47] ILs and salts. It has been shown that the enhanced ability to undergo phase separation is closely related to the decrease on the hydrogen-bond basicity (β)[28,48] depending on the anion. In fact, ILs sharing the $[C_4mim]^+$ cation combined with anions such as $[CH_3CO_2]^-$, $[CH_3SO_3]^-$ and halogens (Cl^- and Br^-) have higher β, presenting a shorter biphasic region, while those paired with $[CF_3SO_3]^-$ and $[N(CN)_2]^-$ present lower β, possessing thus, a higher ability to two-phase formation[45,48]. Moreover, for ILs sharing the $[C_2mim]^+$ cation the same trend is verified, where anions such as, triflate $[CF_3SO_3]^-$ present higher aptitude to form ABS than their halogens (Cl^-) based counterparts[45].

The cation core effect on the aptitude to induce the ABS formation was evaluated using ILs with a common Cl^- anion conjugated with four distinct cations, those differing from being either aromatic or aliphatic: $[C_2mim]^+$, $[OHC_2mim]^+$, $[N_{2,2,2,2}]^+$ and $[Ch]^+$. The

binodal curves are depicted in Fig. 3 and the general ability to perform ABS is reported on Table 1. There seems to be two different driving forces influencing the ABS behaviour: for the imidazolium-based ILs the increasing hydrophobicity from $[C_2mimOH]^+$ to $[C_2mim]^+$ of the cation core moves the binodal curve towards the water-rich region, as well-reported in literature[28,35]; for the ammonium-based compounds ($[N_{2,2,2,2}]Cl$ and [Ch]Cl), a reversed effect is noticed. In this case, $[N_{2,2,2,2}]^+$ represents the most hydrophobic core being however the less able to promote the separation of the phases (contrarily to the well-described trends that indicate that ammonium-based compounds are more efficient at creating ABS than their imidazolium counterparts[27,29]). This indicates that other parameters beyond the hydrophobic nature of the cation are influencing the ABS formation. Meanwhile, most works assessing the impact of the cation core are related with IL/salts-based ABS; when dealing with polymeric ABS containing ILs, the interactions are by far more intricate, and consequently, additional molecular insights are needed.

The effect of electrolyte concentration on the ABS formation was studied by varying the amount of either NaCl and $[C_2mim][N(CN)_2]$ (IL with the highest capacity to promote ABS formation) from 5 wt% to 2.5 wt% and down to 0.1 wt%. The binodal curves determined are depicted in Fig. 5. By increasing the electrolyte concentration (increasing the ionic strength) enhanced capacities to perform ABS are accomplished (Table 1). For higher concentrations of NaCl, the effect is narrower, becoming more significant when its amount is reduced; on the other hand, a more pronounced effect is observed for the IL. Such tendency is in agreement with the results reported by Johansson *et al.*[32] for polymeric ABS using inorganic salts as electrolytes; however concentrations below 1.05 wt% have never been studied. Moreover, in polymer/salt-based ABS containing ILs as adjuvants, the increasing amount of IL enhanced the aptitude to ABS formation, as verified here[39]. Remarkably, the stronger aptitude of NaCl to undergo phase separation compared to $[C_2mim][N(CN)_2]$ can be minimized at lower electrolyte concentrations (*e.g.* 0.1 wt%) opening new perspectives on the use of ILs as electrolytes in polymeric ABS.

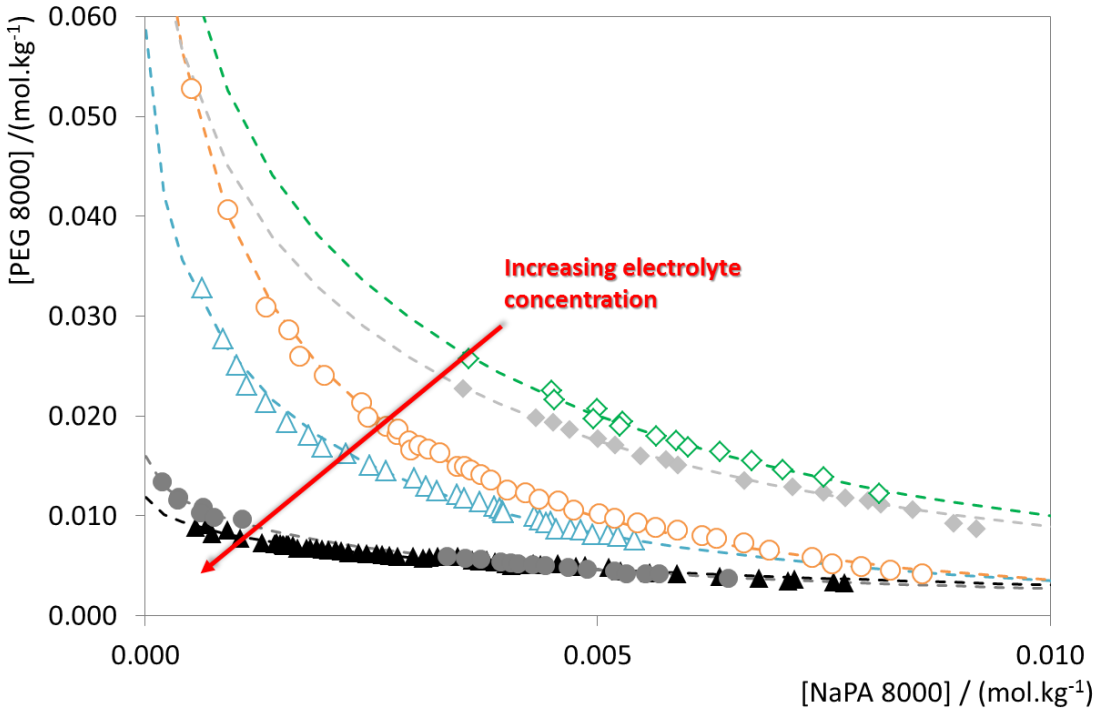

Figure 5. Binodal curves of polymeric ABS at different electrolytes' concentration: 5 wt% of NaCl (▲), 2.5 wt% of NaCl (●), 0.1 wt% NaCl (◆), 5 wt% of [C_2mim][$N(CN)_2$] (△), 2.5 wt% of [C_2mim][$N(CN)_2$] (○) and 0.1 wt % [C_2mim][$N(CN)_2$] (◇). Binodal curves adjusted using Eq. 1 are represented in dashed lines. The arrow is a guide to the eye.

1.3.1.2. Characterization of ILs' partition and media pH

After the determination of the binodal curves which allow the selection of appropriate mixtures at the biphasic region (thus, performing ABS), the understanding of ILs' partition (K_{IL}) as well as the pH of the systems are of utmost importance for the final application, *i.e.* to be used as extraction/purification processes. This was investigated by using the [C_2mim]-based ILs which display maximum absorbance at 211 nm.

In Fig. 6 the K_{IL} along with the pH values of the systems are reported. By the analysis of pH variation with the ILs used as electrolytes, only minor variations from 7 to 8 were observed. Although these systems are not buffered, the pH is kept constant at neutral values, allowing the maintenance of the molecules' charge as constant during the partition experiments. The ILs' partitioning behavior, given by the K_{IL} (Eq. 2), follows the trend [C_2mim][DMP] ≈ [OHC_2mim]Cl > [C_2mim][CH_3SO_3] > [C_2mim][CF_3SO_3] > [C_2mim][CH_3CO_2] > [C_2mim][Tos] > [C_2mim]Cl > [C_2mim][$N(CN)_2$]. It is clear that the IL migrates towards the NaPA-rich phase (K_{IL} > 1), with the exception of [C_2mim][$N(CN)_2$], which is equally distributed among both aqueous phases (K_{IL} = 1). This

preferential migration is easily justified by the electrostatic interactions between the ILs' cation core with the negatively charged species of the polymer – NaPA is negatively charged at neutral pH, due to the presence of carboxylic groups in the main chain. For the specific case of $[C_2mim][N(CN)_2]$, its stronger hydrophobic nature may instigate additional interactions that start to deviate the IL's migration towards the PEG-rich phase. Also in PEG/salt-based ABS using ILs as adjuvants, the nature of the IL dictated the partitioning phenomenon towards either the PEG-rich or the salt-rich phase[39,40].

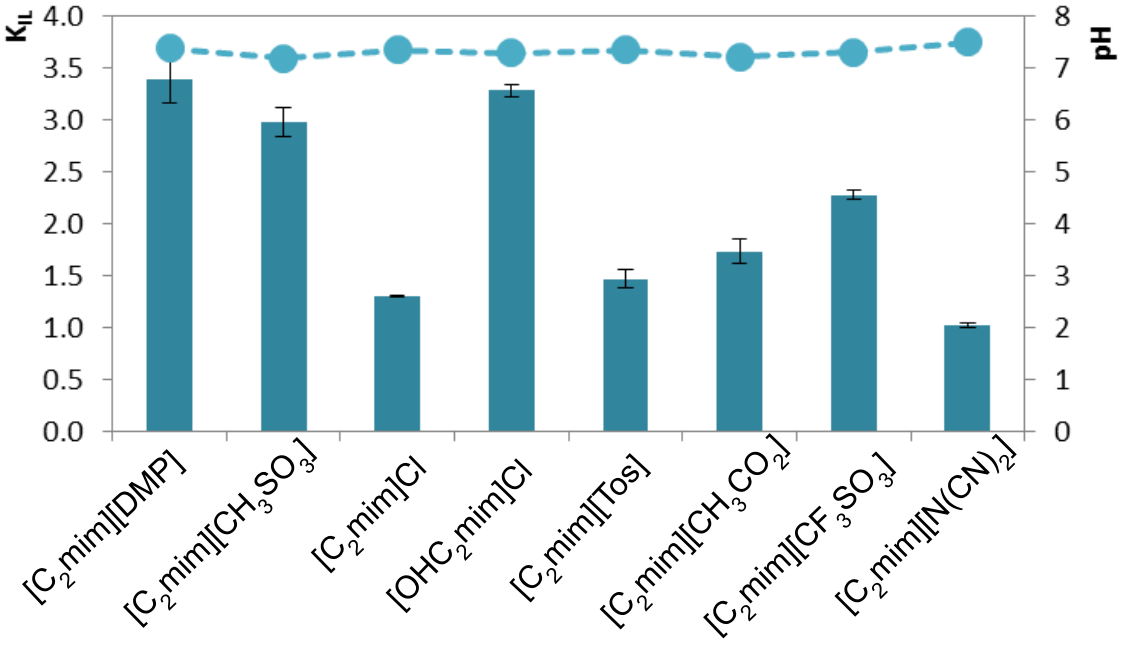

Figure 6. K_{IL} (blue bars) of $[C_2mim]$-based ILs and pH values of the corresponding bottom-phase of the systems (●). The lines are provided just to guide the eye.

1.3.2. Application of the studied ABS as purification platforms

In order to provide the proof of applicability of this novel class of ABS as purification platforms, partitioning studies of two probe molecules, namely CA and Cyt c, were conducted. Those were carried out using ABS composed of 15 wt% PEG 8000 + 4.5 wt% NaPA 8000 + 5 wt% of electrolyte (either ILs or inorganic salts). Due to practical limitations related to the analytical detection of Cyt c content in the bottom phase, it was not possible to determine the $K_{Cyt\ c}$. Thereby, the comparison of the partitioning phenomenon of the target molecules was performed taking into account the EE values.

The EE data attained for CA and Cyt c using the polymeric ABS herein developed are provided in Fig. 7. In fact, high EE values were attained ranging from 80.13 ± 1.45 %

to 97.85 ± 1.37 % for CA for top phase and from 86.23 ± 3.75 % to 100 % for Cyt c for bottom phase. From these results, it is possible to observe the total migration of Cyt c and CA towards opposite directions in all the systems investigated, which demonstrates their selective extraction. For these two compounds, the selectivity is not a crucial point, however, these results suggest that it will be possible to manipulate the selective extraction of similar compounds through, the proper design of the ABS applied. Meanwhile, it is noticed that the protein (a much more complex chemical structure) partitions towards the NaPA 8000-rich phase (bottom phase), while the CA is more concentrated in the PEG 8000-rich phase (top phase). This scenario can be explained based on the balance of interactions and effects occurring between the main components of the aqueous system, which are related with the intrinsic properties of each ABS phase and those of the target molecules (the dissociation curves of the target compounds and the pH values of the coexisting phases of each ABS are provided in Fig. A.1-2 from Appendix A). The partition phenomenon of Cyt c is governed by *"NaPA 8000 – Cyt c"* interactions, since Cyt c is positively charged at pH at around 7 (p*I* ≈ 10.0)[43], giving rise to electrostatic interactions with the charged species of the NaPA 8000. It should be stressed that the presence of electrolytes in NaPA 8000-rich phase (*"Cyt c-electrolyte"* additional interactions) is likely incrementing the strength of such interactions. Conversely, the preferential migration of CA towards the PEG 8000-rich phase seems to be controlled by a balance between, *"PEG 8000-CA"* interactions and, specially, *"NaPA 8000-CA"* repulsive effects. If in one hand, CA displays a logP of 1.22 that indicates a slightly higher preference towards hydrophobic environments (*e.g.* PEG 8000 layer), on the other hand, this dye is negatively charged at neutral pH (pKa of 0.58 and 3.18)[35], being intensely expelled from NaPA-rich phase. Meanwhile, no significant differences with the electrolyte adopted at the level of the extractive performances are observed. Additionally, the K_{CA} values determined for this set of ABS along with additional pictures of each coloured/uncoloured phases (for CA and Cyt c) are provided in Fig.A.4 and Table A.7 from Appendix A, aimed at merely supporting the migration preference observed. In general, the K_{CA}, contrarily to the EE_{CA}, is boosted by the use of inorganic salts (maximum K_{CA} of 10.91 ± 0.41 attained for Na_2SO_4) as electrolytes when compared to ILs (maximum K_{CA} of 4.18 ± 0.29 obtained for [C_2mim][DMP]).

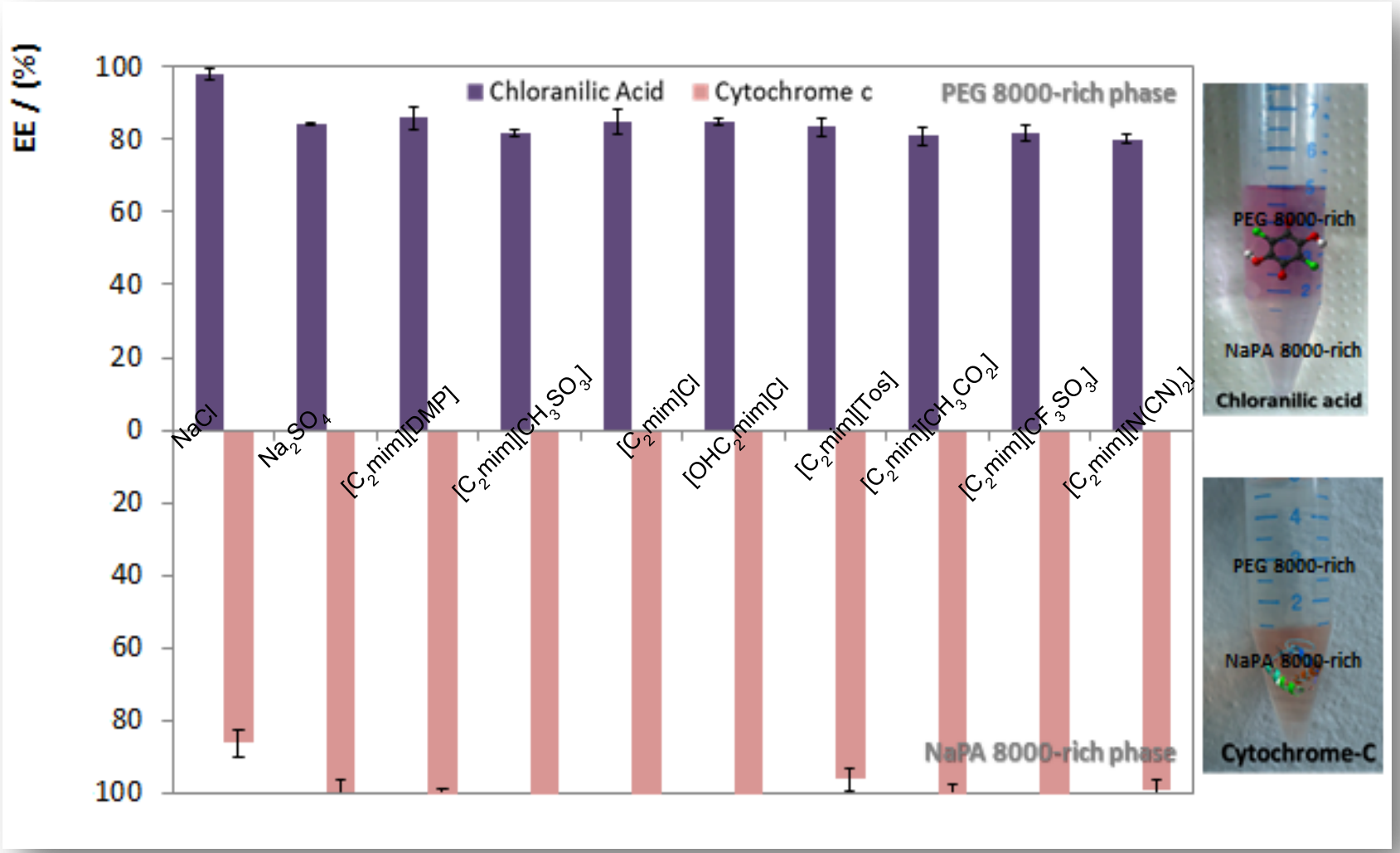

Figure 7. Extraction efficiencies (EE, %) for CA (purple bars) and Cyt c (pink bars) in the ABS composed of 15.0 wt% of PEG + 4.5 wt% of NaPA + 5.0 wt% of electrolytes (inorganic salts or $[C_2mim][X]$). The colour of the phases allows a visual inspection of the migration preferences.

As an attempt to improve the extractive performance of the ABS using ILs as electrolytes, the amount of IL was minimized, ranging from 5 wt%, 2.5 wt% to 0.1 wt%. ABS containing $[C_2mim][N(CN)_2]$ as electrolyte were selected due to the lowest K_{CA} attained (Table A.7 from Appendix A) and availability of the binodal curves at different IL concentration (see section *1.3.1.1. of Results and Discussion*). The results obtained for both K_{CA} and EE_{CA} values are shown in Fig. 8, which clearly indicate that the lowest IL concentration (0.1 wt%) is prompting the CA migration towards the PEG 8000-rich phase (*circa* 5 times more than with the use of 5 wt% of IL). These results indicate that, beyond the *"PEG 8000-CA"* interactions and the *"NaPA 8000-CA"* repulsive effects, also *"CA-ILs"* interactions between the aromatic rings of CA and $[C_2mim][N(CN)_2]$ ($\pi\cdots\pi$ stacking) may occur. At lower IL concentrations, *"CA-ILs"* interactions are much weaker and thus, the repulsive effect of NaPA 8000 upon the dye towards the PEG 8000-rich phase is even stronger, boosting the K_{CA} values. Remarkably, this minimization of IL content causes a significant enhancement at the level of K_{CA} up to 12.44 ± 1.08, which is equivalent or even larger than those obtained with 5 wt% of inorganic salts (10.91 ± 0.41 for Na_2SO_4 and 5.27 ± 0.51 for NaCl). It should be noted that although the trend of the extractive performance with the $[C_2mim][N(CN)_2]$ concentration is scattered, evidences of improvements at lower concentrations are noticed as the EE_{CA} increases *at circa* 10 – 15 % (Fig. 8). From this set of results emerges the idea that lowering the amounts of IL employed as electrolyte, not only the extractive performance, but also the economic and environmental aspects of this class of ABS are improved, encouraging more studies to optimize their behaviour at the molecular level and extraction performance. In fact, these systems can be used in a near future to extract and purify molecules from marine raw materials, by taking advantages of the higher amounts need to promote the ABS formation, by using the water constituting the marine raw materials.

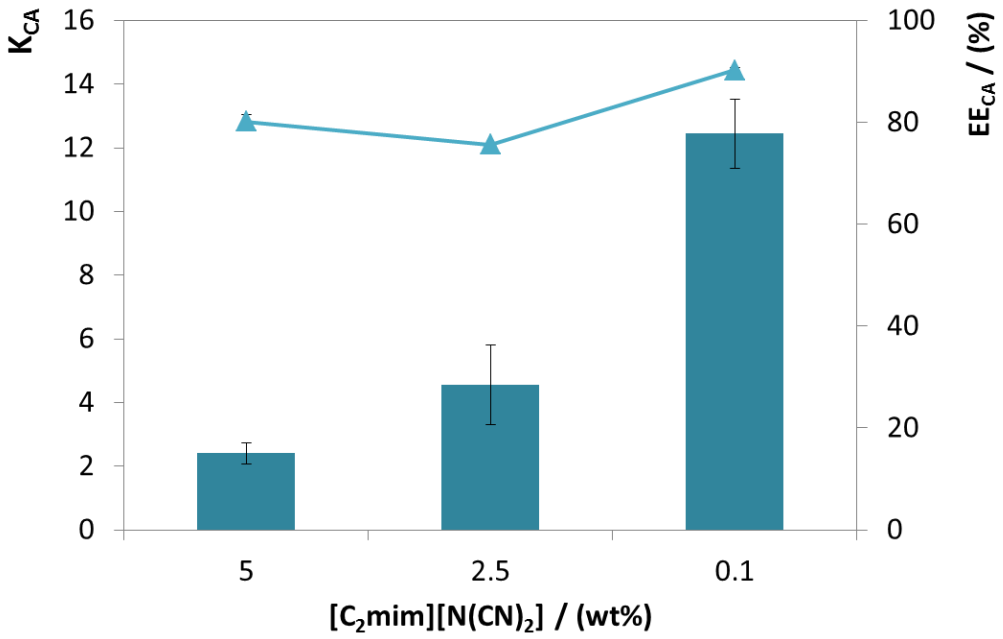

Figure 8. Effect of [C_2mim][N(CN)$_2$] concentration on the partition coefficients, K_{CA} (blue bars) and extraction efficiency data, EE_{CA}, % (▲) of CA.

1.4. Conclusions

In this work, new experimental phase diagrams composed of PEG 8000 + NaPA 8000 + water and several ILs as electrolytes were determined at (298 ± 1) K and atmospheric pressure. Firstly, it is important to remark that this class of ABS reveals great aptitude to undergo phase separation when compared to other classes. The ability of the electrolytes to promote the ABS formation is ruled by the electrolytes' ionic strength, being the inorganic salts (NaCl and Na_2SO_4) more effective than the ILs here investigated. It should be noted that this discrepancy fades at lower concentrations of electrolyte. Considering the IL structural features, the anion moiety effect is well-defined, *i.e.* lower hydrogen-bond basicities induce larger biphasic regions; however, the effect of the cation core is more intricate. When the concentration of electrolyte is taken into account, higher amounts are more beneficial to the ABS formation. In a mixture belonging to the biphasic region of each binodal curve, these systems result in a PEG 8000-rich (top) phase and a NaPA 8000-rich (bottom) phase, for which the IL migrates. The application of these ABS in the extraction of Cyt c and CA revealed an efficient selective process. In other words, Cyt c completely migrated towards the NaPA 8000-rich phase, mainly due to electrostatic interactions, whereas CA was totally expelled towards the PEG 8000-rich phase as a result

of repulsive effects. Within the set of parameters optimized (electrolyte type and concentration, as well as IL structural features), it was possible to significantly improve the extraction parameters by simply lowering the IL concentration down to 0.1 wt%. In this context, both cost and environmental impacts allied with ILs employed as electrolytes are significantly reduced, instigating the creation of more competitive and attractive technologies.

1.5. Future work

A more extensive screening, with other IL families should be accomplished, as an attempt to identify ILs' structures with higher ability of promoting the ABS formation and their actuation mechanism. In this context, two main strategies should be adopted; the first regards the use ILs of more benign nature, namely belonging to the cholinium family while the second considers the application of ILs with tensioactive properties, due to their high hydrophobicity and ability to form micelles. Additionally, the application of these types of ABS should be applied in the extraction of added-value compounds from real matrices, such as fermentation media or marine raw materials.

Aiming at providing further insights into the interactions controlling the partition phenomenon, further partition studies with other molecules should be carried out. Also, in order to understand the mechanisms governing the phase separation, molecular-level studies should be performed, *e.g.* using NMR, COSMO-RS as well as molecular dynamics simulation. Moreover, the investigation of other polymer blends should be carried in the future, not only to validate the applicability of ILs as electrolytes, but also to find more advantageous/effective systems.

Chapter II

Application of ABS as analytical tools in the forensic toxicology field

Abstract

The present work describes two alternative methods to detect benzoylecgonine (cocaine main metabolite) in human urine samples and harmine and harmaline in *Ayahuasca* preparations (*Santo Daime*). The method was based on two stages: the first consists on the sample pre-concentration using ionic liquids-based aqueous biphasic systems (IL-based ABS); the second involves the quantification of the target compounds by HPLC for benzoylecgonine and capillary electrophoresis for two hallucinogens. Both methods were shown to be easy and fast from a practical perspective. However, the data gauged suggest that in both cases, the ABS were not successful in the pre-concentration stage, indicating the need for further studies.

2.1. Introduction

Toxicology is a multidisciplinary science that studies the adverse effects of chemicals on living organisms[49]. One of its most emerging areas is forensic toxicology, which can be defined as the science that works with biological fluid proofs, diagnosing exogenous intoxications, normally related with criminal practices[49,50]. Currently, forensic toxicology is an area in constant change, as new poisons and drugs are daily discovered many of them from the new human lifestyle. Forensic toxicology has been facing constant technological challenges: if in one hand, the new technologies available in analytical chemistry allow more accurate quantification/detection/identification, on the other hand, the constant appearance of novel drugs hampers the creation of standard protocols[50]. The major drawbacks in the forensic field are firstly related with the sample preparation as the sample amount available for analysis is frequently extremely low, the matrices usually present high degrees of complexity and the target compounds are commonly present in trace levels. Moreover, it is likely that the limit of detection (LOD) of the quantification techniques is higher than the amounts of target analyte present in the sample, precluding its quantification. Bearing this in mind, there is an urgent need for more powerful pre-concentration approaches. The sample preparation is currently performed using conventional liquid-liquid extraction (LLE), solid phase extraction (SPE) and purge-and-trap; however, novel extractive approaches such as micro-sample preparation techniques and aqueous biphasic systems based on ionic liquids (IL-based ABS) are being proposed as more advantageous alternatives[51,52]. Despite of the differences between them, such techniques are simple and fast from an operational perspective and require low or even null amounts of volatile solvents.

The first report on IL-based ABS was given by Rogers and co-workers[53] that proved that hydrophilic IL in contact with aqueous solution of a phosphate-based salt can create two aqueous phases, which can be in separation processes, among other possible applications. Since then, several works have been applying distinct ILs, expanding the cation/anion possible combinations to be used, and different salts beyond the phosphate-based ones, as recently reviewed by Freire *et al.*[28]. In fact, the *designer solvent* status[42] given to ILs is relevant in the design of extractive/analytical approaches for a molecule of interest. The applications for IL-based ABS are nowadays vast and versatile ranging from the recovery of drugs from pharmaceutical wastes[47] to the extraction of natural colorants[54]

and lipolytic enzymes[16,55] from fermentation broths. In analytical chemistry, this class of ABS was successfully applied as sample pre-treatment techniques for doping agents[56] and endocrine disruptors[57] from urine or opium alkaloids from *Pericarpium papaveris*[58]. For instance, it is reported that is possible "to concentrate bisphenol A up to 100-fold in one single step procedure using IL-based ABS"[57]. Moreover, the abundant content in water, the non-usage of hazardous organic solvents and the low cost of the experimental apparatus[12] make this an attractive technique for the preparation of sample for forensic purposes.

In this work, IL-based ABS are proposed as alternative routes for sample preparation in what concerns the detection of alkaloids of forensic interest. For that, the first step was the establishment of the experimental ternary phase diagrams for 1-ethyl-3-methylimidazolium ($[C_2mim]$)-based ILs + potassium phosphate tribasic (K_3PO_4) + water systems at (298 ± 1) K and atmospheric pressure. After that, partitioning studies of the alkaloids were conducted using the systems determined with two distinct purposes: the first regards the extraction of cocaine from human urine for further quantification using high performance liquid chromatography (HPLC); the second intends to recover hallucinogens present in tea to be quantified using a novel analytical method based on capillary electrophoresis (CE). In the following sections of the introduction (see *sections 2.1.1* and *2.1.2*) it is provided more detailed information about the alkaloids used in this investigation.

2.1.1. Cocaine and benzoylecgnonine

Cocaine, formally known as benzoylmethylecgonine, is the major alkaloid obtained from the leaves of coca plant (*Erythroxylum coca*). This psychotropic drug has a long history of human use and abuse. It is a stimulant, appetite suppressant and nonspecific voltage gated sodium channel blocker that causes anaesthesia at low doses[59,60]. Cocaine can be introduced into the body by intranasal ("snorting") or intravenous (injecting) entries, oral ingestion, or smoking the free base form (commonly referred to as "crack")[61,62]. According to United Nations World Drug Report (New York, 2013), the global area under coca cultivation amounted to 155,600 ha in 2011. The amounts of cocaine manufactured (expressed in quantities of pure cocaine) were estimated to range from 776 to 1,051 tons in 2011. The world's largest cocaine seizures were reported to take place in Colombia (200

tons) and in the USA (94 tons). The cocaine market seems to be expanding, which leads to massive concerning levels of consumption worldwide.

Cocaine displays several metabolites (Fig. 9); for instance, in 1990 Zhang *et al.*[63] have found 11 metabolites, including four never reported before. The major metabolites of cocaine are easily recognizable and detectable. The degradation of cocaine into its metabolites is a result either from hydrolysis or oxidation biochemical reactions. Cocaine (A) in Figure 9 is oxidized by specific cytochromes P450 (CYPs) and N-demethylated to into norcocaine (B). It can be further oxidized into N-hydroxy cocaine (C), a low probable metabolite, by oxidative metabolism. Benzoylecgonine (D) and ecgonine methyl ester (E) are formed from the ester cleavage hydrolytic reaction of cocaine by serum cholinesterases and hepatic carboxylesterases. Further hydrolysis of these compounds leads to the formation of ecgonine (F), another major metabolite[59,60].

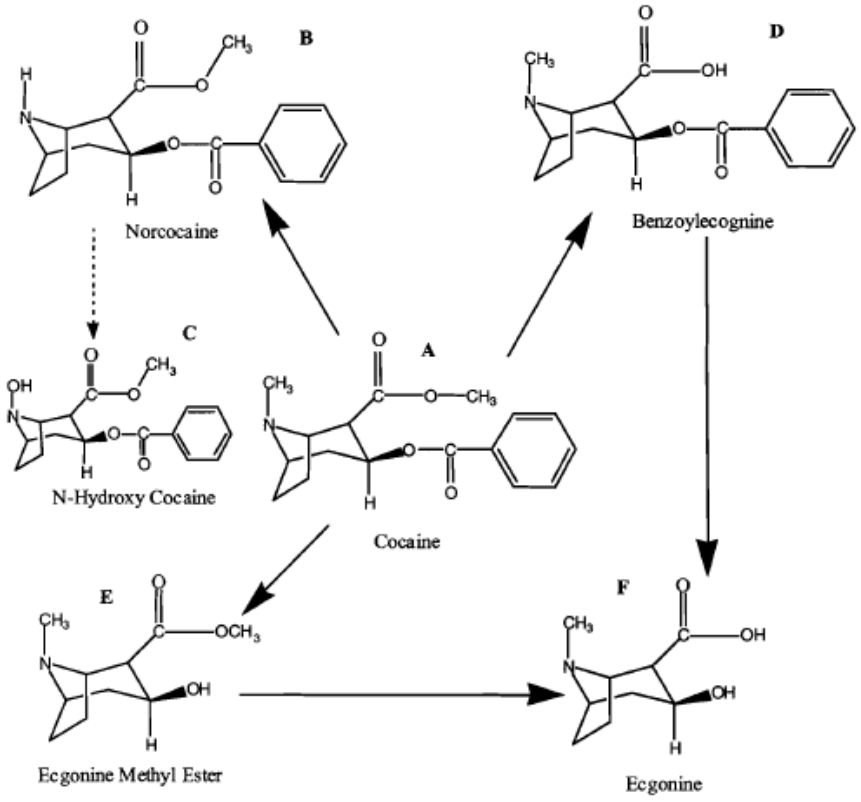

Figure. 9 Cocaine and its primary metabolites, including benzoylecgonine (BE)[64].

Around 86-90% of an administered dose of cocaine is recovered in urine as either cocaine (only 1-5 %) or one of its metabolites. Among the degradation metabolites, benzoylecgonine is the one provided of major toxicological and analytical importance.

This is mainly due to the fact that it presents longer half-live than cocaine[65] and consists of 46% of the excreted metabolites[59]. However, its content in urine is in the order of $ng.mL^{-1}$ units, which represents a limiting step for the accurate quantification of this metabolite.

Recently, many studies have been carried out with the aim of improving drug detection present in samples of human origin, such as hair[66–69], urine[64,70–75] and blood[69,73,74,76,77]. This is highly important for a comprehensive set of applications, namely drug abuse studies, analysis in forensic toxicology, drug use monitoring in workplace and doping control in competitions. Several research works have been dealing with the development of analytical methods for drug detection in samples from human origin. Most of these studies use solid-phase extraction (SPE)[67,68,75,78] as sample preparation method. Meanwhile, the detection or quantification of cocaine and/or respective metabolites present in diverse samples is mainly conducted by using gas chromatography coupled with mass spectrometry (GC–MS)[66,72,74] and high performance liquid chromatography (HPLC) with UV detection [71,75]. However, for GC-MS analysis the sample must be derivatizated, what introduces an additional cost to the method. Moreover, both SPE and GC–MS are time-consuming techniques, which use higher volumes of hazardous chemicals (*e.g.* organic solvents) and require a lot of sample manipulation. Additionally, few studies on SPME application in benzoylecgonine extraction from urine[72] and hair[66] appeared.

2.1.2. Harmine and harmaline

Ayahuasca, also known by the names Hoasca, Daime, Yajé, Natema and Vegetal, is a psychoactive tea plant originally used by shamans in the Amazon Basin in magical-religious practices and folk medicine of indigenous people[79,80]. This beverage is obtained by infusing the powdered stems of *Banisteriopsis caapi* in combination with the leaves of *Psychotria viridis*. *Psychotria viridis* contains the psychedelic agent called N,N-dimethyltryptamine (DMT), whereas *B. caapi* contains β-carbolines such as harmine, harmaline and tetrahydroharmine, which are potent monoamine oxidase (MAO) inhibitors. Dimethyltryptamine is not orally active itself, since it is inactivated by peripheral MAO present in liver and gut. However, the inhibition of MAO by β-carbolines allows the oral activity of dimethyltryptamine, enabling its action towards the central nervous system. The synergistic interaction of these alkaloids is the basis of the psychotropic action of *Ayahuasca*[81]. In Brazil, *Ayahuasca* has been incorporated in rituals of modern syncretic

religious groups, mainly the Santo Daime and the União do Vegetal (UDV), where the beverage is reported to be used to facilitate self-knowledge and introspection. In 2004, the use of *Ayahuasca* within religious context was officially recognised and protected by law in Brazil (Conselho Nacional Antidrogas Brasil, 2004). Up to date, Brazil is the only country where it is held under legal protection, analogous to the status of peyote (*Lophophora williamsii*) usage in the United States[82]. The use of *Ayahuasca* has spread outside South America, being now established in the United States and in Europe [80]. With the increasing consumption of such psychotropic tea, this beverage has begun to attract the attention of researchers in what regards its pharmacological and toxicological aspects[79–84].

In the last years, several authors have devoted their attention in the characterization of the *Ayahuasca* alkaloids' profile. The peruvian *Ayahuasca* (100 mL) was shown to contain dimethyltryptamine (60 mg), harmine (467 mg), harmaline (41 mg) and tetrahydroharmine (160 mg), being this characterization achieved through two-dimensional thin-layer chromatography, HPLC and GC-MS[84]. On its turn, the composition of Brazilian *Ayahuasca* (100 mL) has been shown to comprise 24, 170, 20 and 107 mg of the same alkaloids, respectively, using GC and HPLC[85].

Among the vast number of analytical techniques that can be used in the forensic toxicology field, capillary electrophoresis (CE) arises as one of the most important tools in the screening and quantification of illicit drugs, bio-transformed products and other forensic medicines. In fact, a huge number of articles regarding the CE application in the quantification of several drugs can be found in literature[37-45]. In the last years, the widely applied separation and quantification techniques HPLC and GC-MS, has been looked with minor interest, largely because of the lack of applicability in forensic toxicology. It is when CE gains considerable attention, due to the higher separation power (up to millions of theoretical dishes), rapid analysis time, high mass sensitivity and low cost associated (small sample volumes required and consumables)[69,86]. This technique is also provided of considerable flexibility from both separation mode (*e.g.* electrophoretic, electrokinetic chromatography) and detection (*e.g.* UV-visible, fluorescence, conductivity, mass) points of view[86–94]. Micellar electrokinetic chromatography (MEKC) was adopted during this work for the quantification of harmine and harmaline extracted from tea with IL-based ABS. This technique is based on a mobile phase (buffer) containing a surfactant, commonly sodium dodecyl sulfate (SDS). The presence of a surfactant induces the creation

of micelles, allowing the analytes to be distributed between the hydrophobic interior of the micelle and the hydrophilic buffer solution. To enable the quantification of these hallucinogens aroused the need for the development and validation of a new analytical method.

2.2. Material and methods

Phase diagrams of IL/K_3PO_4-based ABS

2.2.1. Materials

The ILs used in this chapter of the present thesis were [C_2mim]Cl, [C_2mim][DMP], [C_2mim][CH_3SO_3], [C_2mim][Tos], [C_2mim][CH_3CO_2], [C_2mim][CF_3SO_3], [C_2mim][$N(CN)_2$] and [$N_{2,2,2,2}$]Br. Their suppliers, purities, full name and chemical structures are reported on Chapter 1, *Section 1.2.1*. The salt potassium phosphate tribasic K_3PO_4 (97 wt%) was purchased from Sigma-Aldrich®. The water used was double distilled, passed by a reverse osmosis system and further treated with a Milli-Q plus 185 water purification apparatus.

2.2.2. Experimental determination of phase diagrams

In order to complete the series of ABS studied in the present work, the experimental ternary phase diagrams for the systems composed of several [C_2mim]-based ([C_2mim]Cl, [C_2mim][DMP], [C_2mim][Tos], [C_2mim][CH_3CO_2], [C_2mim][CF_3SO_3], [C_2mim][$N(CN)_2$]) and [$N_{2,2,2,2}$]-based ([$N_{2,2,2,2}$]Br) ILs + K_3PO_4 (pH ≈ 13) + water were determined at (298 ± 1) K and atmospheric pressure. The cloud point titration method was elected in order to determine the experimental binodal curves, following a general experimental procedure already established in previous works[45]. Aqueous stock solutions *at ca.* 80 wt% of each IL and *at ca.* 50 wt% K_3PO_4 (pH ≈ 13) were prepared. Drop-wise addition of the aqueous solution of K_3PO_4 was performed to the IL aqueous solution until the visual perception of a cloudy point (biphasic region). Alternate drop-wise addition of water until the appearance of a clear solution (monophasic region) was then conducted. The experimental solubility curves were correlated using the Merchuk equation[46]:

$$[IL] = A\ exp[(B \times [K_3PO_4]^{0.5}) - (C \times [K_3PO_4]^3)] \quad \textbf{(5)}$$

where [IL] and [K_3PO_4] represent, respectively, the IL and K_3PO_4 mass fraction percentages, and *A*, *B* and *C* are the constants obtained by the regression of the experimental binodal data.

Benzoylecgnonine

2.2.3. Materials

Benzoylecgonine (Fig. 9) free base standard, 1 mg.mL^{-1} in methanol, was obtained from Sigma-Aldrich®. Urine samples from human origin were collected from a non-drug consumer and stored at -20ºC, until they were processed for further extraction and quantification. HPLC grade methanol was acquired at Merck® and ammonium acetate (purity = 99 %) was retrieved from Sigma-Aldrich®.

2.2.4. Benzoylecgonine extraction using IL/K_3PO_4-based ABS

ABS of 5 g of total weight were prepared gravimetrically using glass vials by adding 40 wt% of [$N_{2,2,2,2}$]Br (herein adopted as model IL) + 15 wt% of K_3PO_4 + 45 wt% of human urine samples spiked with 100 µL of the solution of benzoylecgonine in methanol (to obtain a final concentration of 2 ppm of benzoylecgonine in the total ABS volume). At the end, the selected mixtures were able to undergo two phases separation, in with a top phase richer in [$N_{2,2,2,2}$]Br and a bottom phase richer in K_3PO_4. At this time, the phases were carefully separated and collected for the measurement of their weight (uncertainty of ±10^{-4} g), volume and pH. The pH of both IL-rich and salt-rich phases was measured using a Mettler Toledo S47 SevenMulti™ dual meter pH/conductivity equipment with an uncertainty of ±0.02.

2.2.5. HPLC quantification of benzoylecgnonine

The quantification of benzoylecgnonine was assayed by HPLC analysis. A liquid chromatograph consisted of an automatic sampler, pump and diode array detector (DAD). The analytical column adopted was Luna® 5 µm C18 100 Å with dimensions of 250 x 4.6 mm (Phenomenex). The procedure adopted was that previously reported by Clauwaert *et al.*[75], in which the separation was carried out by gradient elution. The mobile phase was composed of 0.045 M ammonium acetate buffer solution (pH 6.5) and methanol. The

phase components were degassed prior to use. The program of elution was conducted according to 0 – 30 min from 10 to 60 % of methanol, 30 – 32 min from 60 to 10 % of methanol and 32 – 40 min 10 % of methanol. The operation flow-rate was 1 $mL.min^{-1}$ and the injection volume was 10 μL. DAD detector was set to record the UV spectra and to measure the column eluent at 241 nm. The identity of benzoylecgnonine was assessed through a comparison of the retention time (24.3 min) and UV spectra obtained for urine (benzoylecgnonine at a concentration of 2 ppm in total ABS volume) to those attained for standard samples (benzoylecgnonine at a concentration of 100 ppm).

Harmine and harmaline

2.2.6. Materials

The pure standards of the alkaloids harmaline hydrochloride dihydrate (purity = 95%) and harmine (purity = 98%) - chemical structures are in Fig. B.1 from Appendix B - were both purchased from Sigma-Aldrich®. The alkaloid powders were dissolved in methanol (analytical-reagent grade) at a concentration of 1 $mg.mL^{-1}$ and stored at 4 ºC under light-protected conditions. *Ayahuasca* preparations were obtained from a religious group settled in the city of Araçoiaba da Serra, State of São Paulo, Brazil (Fig. 10).

For capillary electrophoresis, the MEKC buffer consisted in sodium tetraborate (TBS) from Synth® and sodium dodecyl sulphate (SDS) acquired from Sigma-Aldrich®. Methanol was obtained from Sigma-Aldrich® with high purity grades.

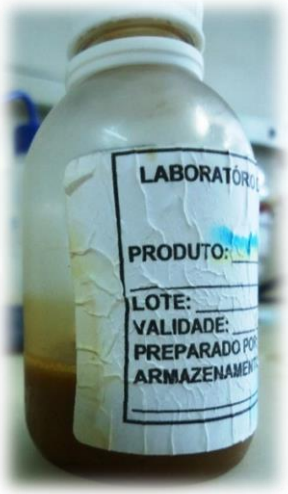

Figure 10. *Ayahuasca* sample.

2.2.7. *Ayahuasca* pre-treatment

Ayahuasca was diluted with Milli-Q water (1:2) and posteriorly centrifuged at 16000 x *g* for 10 minutes at room temperature. The resulting pellet was discarded, being then the supernatant filtered under vacuum using membrane filters (pore size of 0.45 μm) (Fig. 11 and 12). The aqueous supernatant obtained was further used in the ABS extraction experiments.

Figure 11. Filtration paper with fine particles retained (pore size of 0.45 μm).

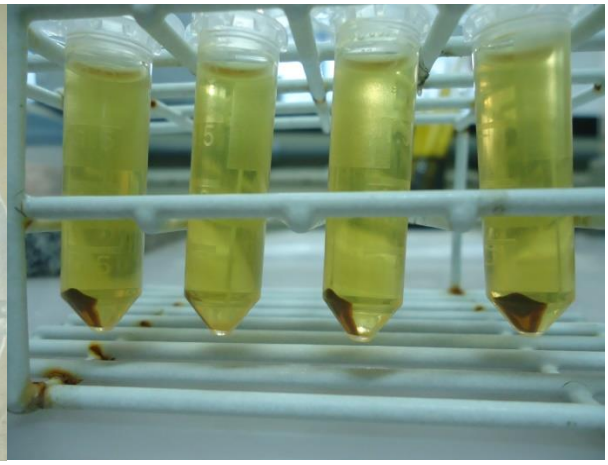

Figure 12. Centrifuged extract with brown solid contaminant pellets.

2.2.8. ABS extraction of hallucinogens from *Ayahuasca*

Two types of ABS were performed to extract harmaline and harmine from *Ayahuasca* supernatant solution: $[C_2mim]Cl/K_3PO_4$-based ABS and PEG 8000/NaPA 8000-based ABS with $[C_2mim]Cl$ as electrolyte. The $[C_2mim]Cl/K_3PO_4$-based ABS were prepared gravimetrically using glass vials by adding 40 wt% of $[C_2mim]Cl$ + 15 wt% of K_3PO_4 + 45 wt% of *Ayahuasca* aqueous supernatant completing a total weight of 5 g. These systems result in two phases, being the IL-rich and the salt-rich phases represented as the top and the bottom layers, respectively. In its turn, polymeric ABS (for further details see Chapter 1) were composed of 15 wt% of PEG 8000 + 4.5 wt% of NaPA 8000 + 5.0 wt% of $[C_2mim]Cl$ + 75.5 wt% of *Ayahuasca* aqueous supernatant fulfilling a total weight of 5 g. Two phases clearly occur, being the PEG 8000 more concentrated in the top phase, while NaPA 8000 mostly appears in the bottom phase. The phases of both types of ABS were carefully separated and collected for the measurement of their weight

(uncertainty of ± 10^{-4} g), volume and pH. The pH was assessed using a Mettler Toledo S47 SevenMulti^{TM} dual meter pH/conductivity equipment with an uncertainty of ± 0.02.

2.2.9. Capillary electrophoresis quantification of hallucinogens

MEKC buffer was freshly prepared and consisted of 20 mM of TBS (pH 9.40), 40 mM of SDS, containing 10% (v/v) methanol. It should be stressed out that an optimization study was performed, being other conditions tested, as described along the text. The buffers were filtered (0.4 μm filters) and kept at 4 ºC prior to be used.

MEKC was performed on the P/ACE 5050 system (Beckman) (Fig. 13) in the normal-polarity mode (positive potential at the injection end of the capillary). The temperature was set at 298 (± 1) K and UV absorbance was monitored at 336 nm using DAD (Beckman Instruments, CA, USA). Peak identity was confirmed by post-run DAD analysis of the maximum absorption of the individual peaks in a mixture of both standards. An unmodified fused-silica capillary (J&W Scientific) was used for all analysis. The capillary has the following dimensions 20 cm effective length × 50 μm internal diameter. Prior to analysis, it was conditioned with 5 volumes of NaOH, 10 volumes of Milli-Q water and 20 volumes of MEKC buffer and it was then subjected to voltage equilibration for 10 minutes until the accomplishment of a stable baseline. Samples' introduction was performed by pressurised injection (0.5 psi, 30 s). Separations were conducted under constant electric current (70 μA, 15 minutes). Between analysis, the capillary was washed for 10 minutes with NaOH, 10 minutes with Milli-Q water and then 15 minutes with the MEKC buffer.

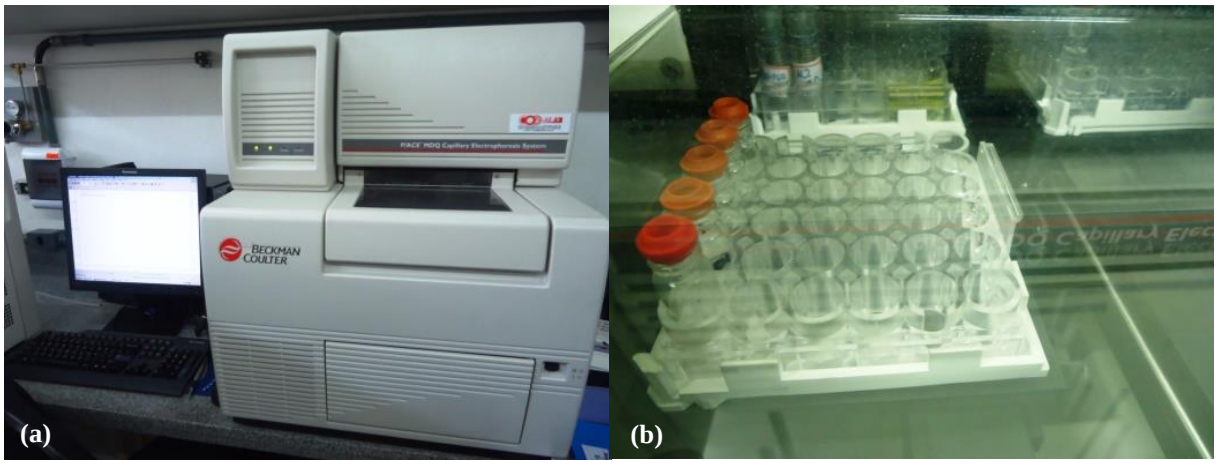

Figure 13. (a) Capillary electrophoresis equipment P/ACE 5050 system (Beckman) (b) Detailed view of microtubes containing the *Ayahuasca* samples.

2.3. Results and Discussion

2.3.1. Analysis of the Phase Diagrams

Ventura *et al.*[45] reported the phase behaviour of ternary systems composed of $[C_2mim]$-based ILs + K_3PO_4 + H_2O. Herein, a complementary study was carried out aimed at incrementing the series of anions ($[Tos]^-$, Cl^-, $[DMP]^-$, $[CH_3CO_2]^-$, $[CF_3SO_3]^-$and $[N(CN)_2]^-$) and cations ($[N_{2,2,2,2}]^+$) available for this strong salting-out agent (stronger salting-out agents are more prone to promote the re-concentration of diverse analytes[57]). The experimental binodal curves adjusted by the Merchuk equation were plotted in Fig. 14 in units of molality (mole of solute *per* kg of solvent) to eliminate possible interferences caused by the discrepancies on the ILs' molecular weight on the binodal curves behaviour. The detailed experimental weight fraction data, respective correlations (adjusted parameters *A*, *B* and *C*) and phase diagrams in mass fraction units are represented in Table B.1-3 and Fig. B.2-3 from Appendix B. The binodal curves established allowed the comparison among the effect of different anion moieties (with ILs sharing either the $[C_2mim]^+$ or the $[N_{2,2,2,2}]^+$ cations).

In what regards the anion effect on the ABS formation, their ability to induce phase separation can be ranked as follows:

$[C_2mim]$-based ILs: $[CF_3SO_3]^- \approx [Tos]^- > [N(CN)_2]^- \approx [DMP]^- > [CH_3CO_2]^- \approx Cl^-$

These results are in good agreement with the whole set of evidences found in literature for the IL's anion effect on the ABS formation[45,47,95]. This is typically correlated based on the capability to create water-ions hydration complexes, which depends on the β of the anions. In other words, anions with lower β values display lower abilities to form coordinative bonds and therefore are more easily salted-out by K_3PO_4, which is translated into extended biphasic regions. As aforementioned, the trend for the anions performance when ILs are working as electrolytes in polymeric ABS (see Chapter 1) is also in good agreement with such findings.

Concerning the cation core impact on the creation of ABS, it is possible to generally conclude that the system containing the quaternary ammonium $[N_{2,2,2,2}]^+$ is more prone to undergo phase separation than the one composed of $[C_2mim]^+$. This is well-reported on literature[27,95], being the phenomenon occurring behind attributed to the higher molar volume and inherent higher hydrophobicity of ILs containing the acyclic cation cores, such as $[N_{2,2,2,2}]^+$.

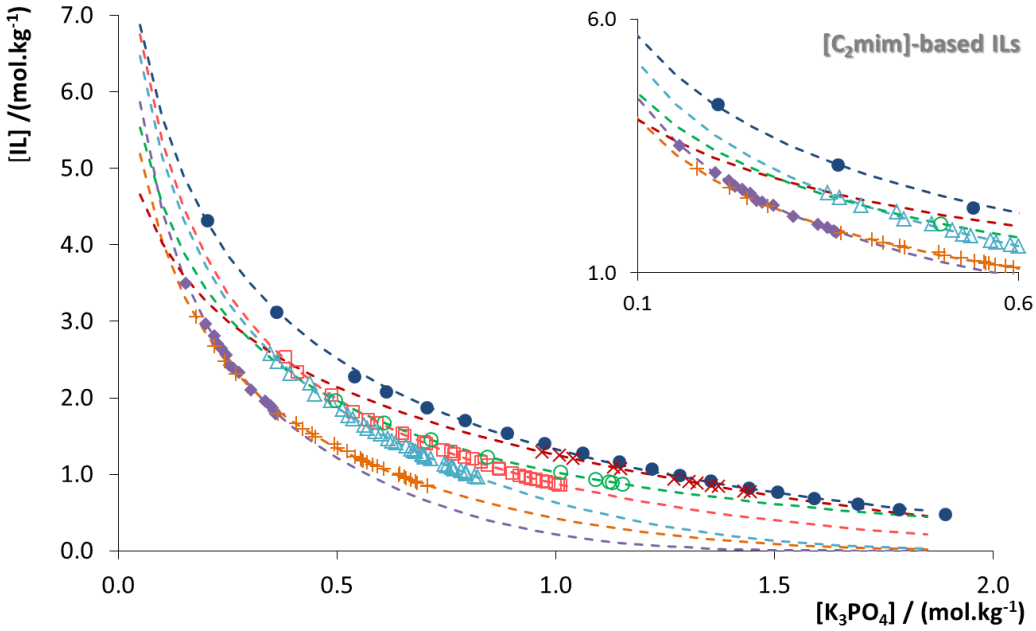

Figure 14. Binodal curves of the IL/K_3PO_4-based ABS: [C_2mim]Cl (●), [C_2mim][CH_3CO_2] (×), [$N_{2,2,2,2}$]Br (□), [C_2mim][DMP] (○), [C_2mim][$N(CN)_2$] (△),[C_2mim][Tos] (+), [C_2mim][CF_3SO_3] (◆) + K_3PO_4 at (298 ± 1) K. Binodal curves adjusted using Eq. 5 are represented in dashed lines. The influence of IL's structural features is provided separately in the insets to simplify the analysis.

2.3.2. Benzoylecgnonine extraction

HPLC is a well-established method to quantify benzoylecgnonine from diverse sources and matrices. Moreover, the use of IL-based ABS as sample pre-treatment approach was already proven to be compatible with the use of HPLC as the quantification technique[58]. The liquid chromatogram shown in Fig. 15 depicts the benzoylecgnonine standard peak (at 100 ppm), with a retention time (RT) of 24.3 min. This peak will be compared to that obtained for each of the coexisting phases, in order to identify and quantify this drug in human urine samples. In this sense, ABS with human urine containing the target drug and the respective blank controls were prepared. Figs. 16 and 17 display the chromatograms for top and bottom phases, respectively of either the drug-containing system or the control. The obtained chromatograms indicate that both blank and extraction systems present a similar profile (for top and bottom phases), with the absence of the benzoylecgnonine peak (RT = 24.3 min). Therefore, as the benzoylecgnonine concentration in the spiked urine is extremely low, the gathered data suggest that the ABS conditions here investigated were not suitable to develop a proper pre-concentration method for benzoylecgnonine; in fact, the target drug concentration remained below the

LOD of the analytical technique. It should be pointed out that the trace amounts of benzoylecgnonine applied are within the levels normally found in human fluids. Also, the strong alkaline environment inherent to the K_3PO_4 presence (pH = 13) can affect benzoylecgonine stability[77].

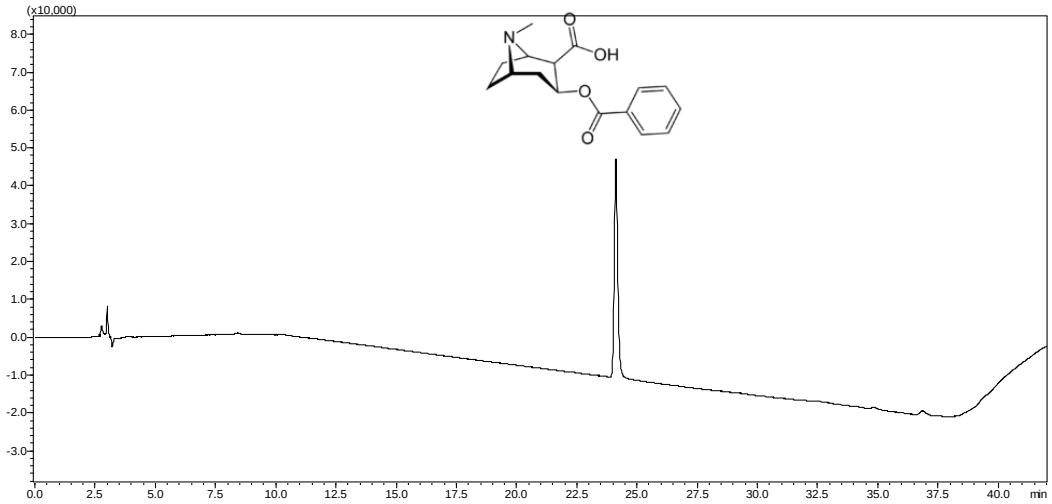

Figure 15. Liquid chromatogram of benzoylecgonine standard (100 ppm).

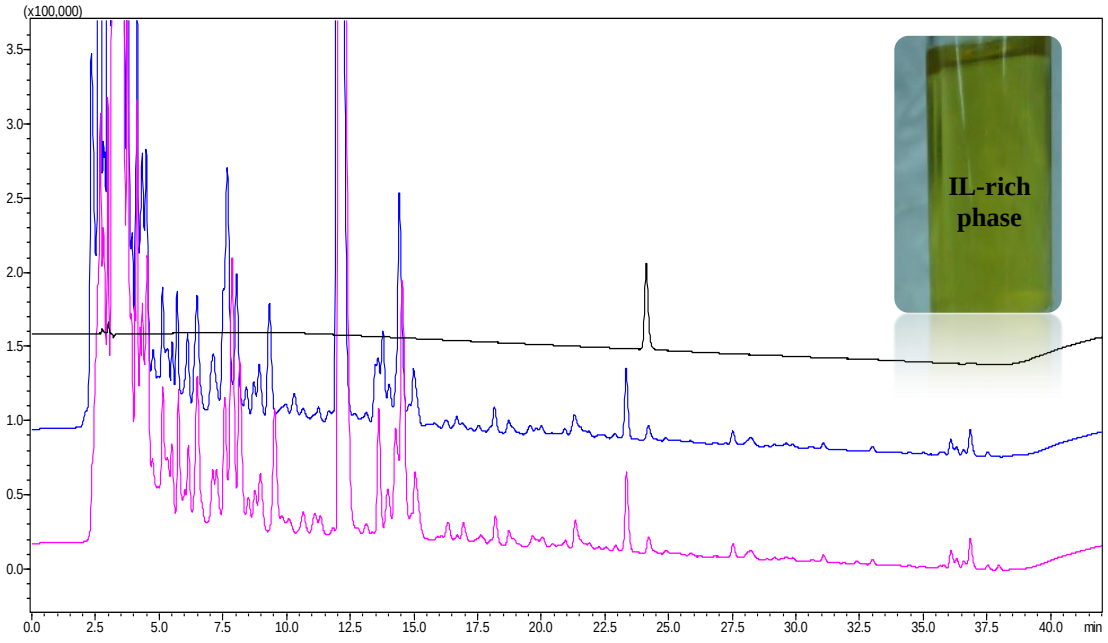

Figure 16. HPLC chromatogram of the benzoylecgonine standard (black line), of the IL-rich phase of blank human urine-based ABS (blue line) and of the IL-rich phase of drug-containing human urine-based ABS (violet line).

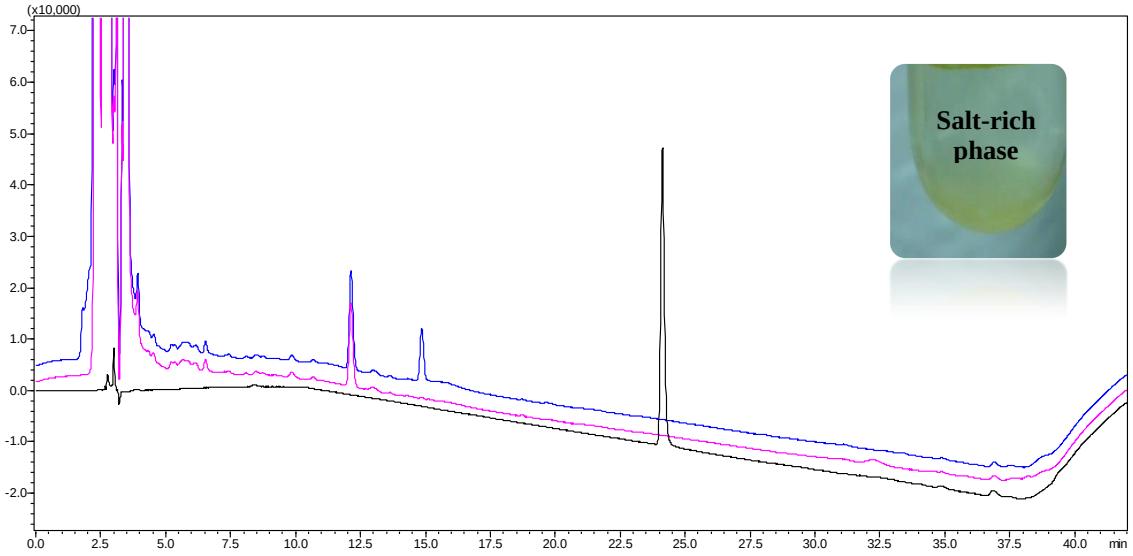

Figure 17. HPLC chromatogram of the benzoylecgonine standard (black line), of the salt-rich phase of blank human urine-based ABS (blue line) and of the salt-rich phase of drug-containing human urine-based ABS (violet line).

2.3.3. Harmine and harmaline extraction

In order to assess the applicability of IL-based ABS as sample pre-treatment/concentration of hallucinogens present in tea, it was necessary to develop and validate a novel MECK method. In this context, two main steps were performed: first, the establishment of MECK method conditions and second, the determination of the calibration curves. Fig. 18 depicts an eletropherogram of an approximately equimolar mixture of both alkaloids standards separated in an alkaline MEKC buffer containing 20 mM of sodium tetraborate, TBS (pH 9.40), 40 mM SDS, 10 % (v/v) methanol across a 20 cm long capillary. Each of the alkaloids could be resolved to base-line in less than 6 minutes. The order of migration was harmine followed by harmaline, being in agreement with the elution times for the single compounds in mixture. These migration times (4.75 min for harmine and 5.05 min for harmaline) were significantly smaller and better resolutions were obtained than in a previous study[96]. This difference is likely a direct cause of the MEKC buffer herein adopted. In order to quantify both alkaloids, calibration curves were previously determined showing linearity over the specified range (80-120 ppm): harmine ($y = 93.74x + 2570$; $R^2 = 0.9541$) and harmaline ($y = 478.2x – 1450$; $R^2 = 0.9811$), where y and x represent the relationship between the peak area of the internal standard and

the corresponding calibration concentrations, respectively. Each standard was analysed in triplicate and the central point concentration was assessed ten times (100 ppm).

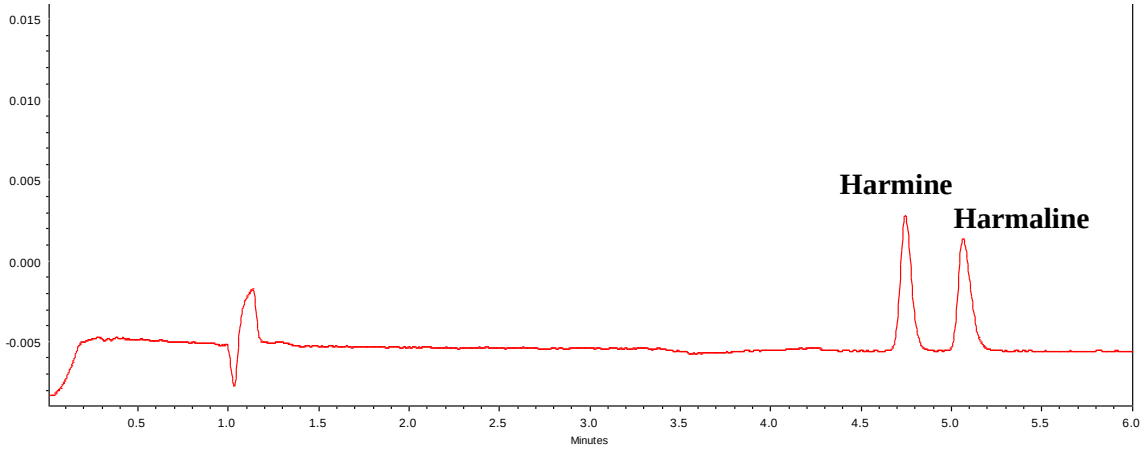

Figure 18. Electropherogram of harmine and harmaline (100 ppm). Conditions: MEKC buffer containing 20 mM sodium tetraborate, TBS (pH 9.40), 40 mM SDS, 10 % (v/v) methanol. Capillary 20 cm to the detector and 50 μm i.d. , Applied current: 70 μA, hydrodynamic injection 0.5 psi for 30 seconds, T = (293.1 ± 0.1) K, at a wavelength of 336 nm.

After properly developing and validating the MEKC method, the pre-treated preparation of hallucinogens from Ayahuasca was extracted by $[C_2mim]Cl/K_3PO_4$-based ABS and PEG 8000/NaPA 8000-based ABS with $[C_2mim]Cl$ as an electrolyte (Fig. 19). From visual analysis of Fig. 19, it is notorious that PEG 8000/NaPA 8000-based ABS exhibit lighter colour of top and bottom phase; this may indicates that less precipitation was obtained in this extraction due to the milder conditions of the separation (higher water content: 75.5 wt% *vs.* 45 wt%). Moreover, the darker aspect of the PEG 8000-rich phase may suggest that the hallucinogens are migrating towards this more hydrophobic phase; this is highly relevant as this type of ABS may be suitable to perform a pre-concentration stage of hallucinogens from aqueous media (tea matrix). However, the obtained electropherograms for the coexisting phases of each type of ABS (Figs. 20 to 23) do not provide quantitative/qualitative proofs. From the electropherograms of $[C_2mim]Cl/K_3PO_4$-based ABS coexisting phases (Figs. 20 and 21), it is possible to notice the presence of several overlapping peaks, precluding the identification and quantification of harmine and harmaline. On the other hand, no peaks were observed in the phases composing the polymeric ABS, impeding again the identification and quantification of both hallucinogens. Yet, the composition of *Ayahuasca* preparation is unknown, making harder to understand the profiles obtained in the electropherograms. Although the MEKC method

was successfully applied to quantify with good resolution harmine and harmaline standards, its application in complex matrixes is a challenge, bringing the need for further studies for characterization of *Ayahuasca* preparation and other quantification methods.

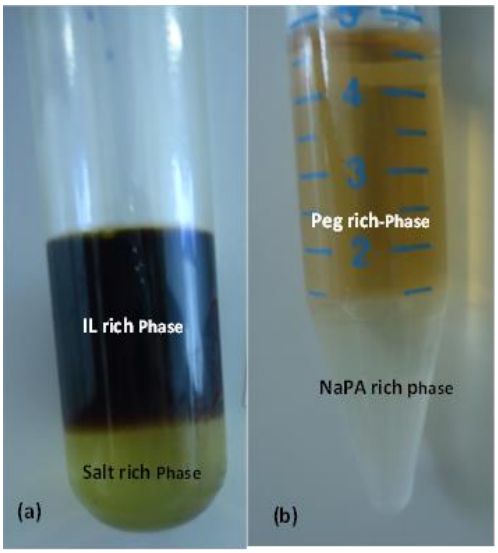

Figure 19. (a) [C_2mim]Cl/K_3PO_4-based ABS extraction of hallucinogens from *Ayahuasca* pre-treated sample, in which [C_2mim]Cl and K_3PO_4 are the top and bottom phases, respectively. (b) PEG 8000/NaPA 8000-based ABS extraction of hallucinogens from *Ayahuasca* pre-treated sample, in which PEG 8000 and NaPA 8000 are the top and bottom phases, respectively.

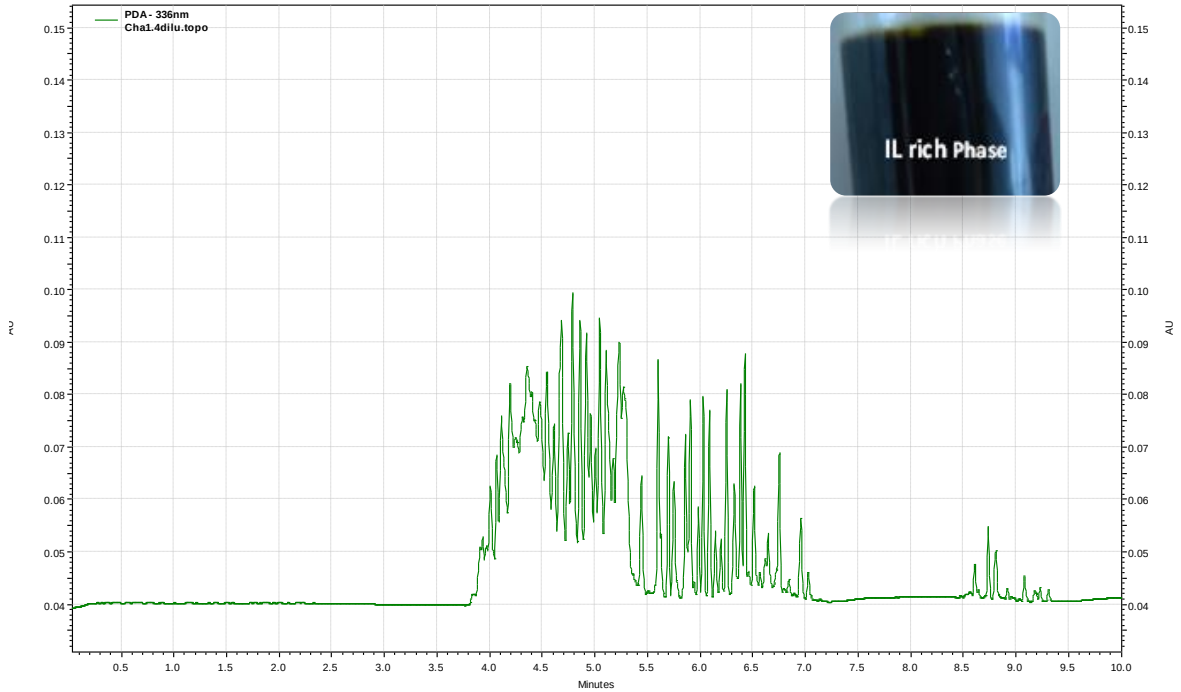

Figure 20. Electropherogram of IL-rich phase of [C_2mim]Cl/K_3PO_4-based ABS prepared using the *Ayahuasca* pre-treated sample. Conditions applied: MEKC buffer containing 20 mM sodium tetraborate, TBS (pH 9.40), 40 mM SDS, 10 % (v/v) of methanol. Capillary 20 cm to the detector and 50 μm i.d., Applied current: 70 μA, hydrodynamic injection 0.5 psi for 30 seconds, T = (293.1 ± 0.1) K, wavelength 336 nm.

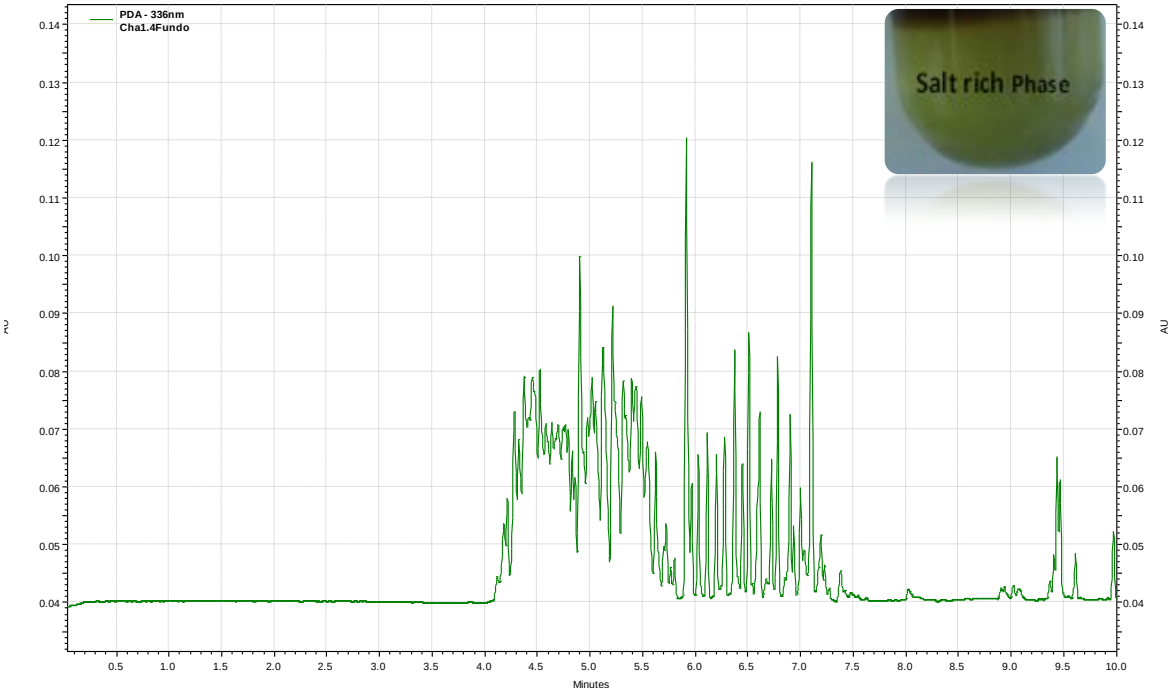

Figure 21. Electropherogram of salt-rich phase of [C_2mim]Cl/K_3PO_4-based ABS prepared using the *Ayahuasca* pre-treated sample. Conditions applied: MEKC buffer containing 20 mM sodium tetraborate, TBS (pH 9.40), 40 mM SDS, 10 % (v/v) of methanol. Capillary 20 cm to the detector and 50 µm i.d., Applied current: 70 µA, hydrodynamic injection 0.5 psi for 30 seconds, T = (293.1 ± 0.1) K, wavelength 336 nm.

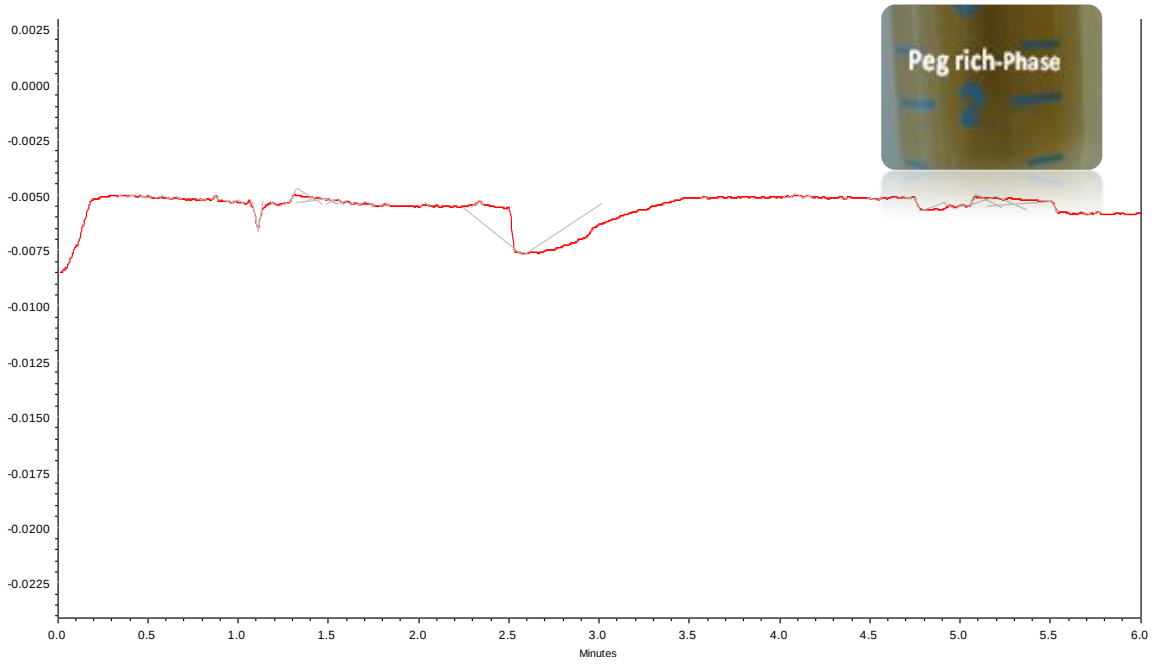

Figure 22. Electropherogram of PEG 8000-rich phase of PEG 8000/NaPA 8000-based ABS with [C_2mim]Cl as electrolyte prepared using the *Ayahuasca* pre-treated sample. Conditions: MEKC buffer containing 20 mM sodium tetraborate, TBS (pH 9.40), 40 mM SDS, 10 % (v/v) of methanol. Capillary 20 cm to the detector and 50µm i.d., Applied current: 70 µA, hydrodynamic injection 0.5 psi for 30 seconds, T = (293.1 ± 0.1) K, wavelength 336 nm.

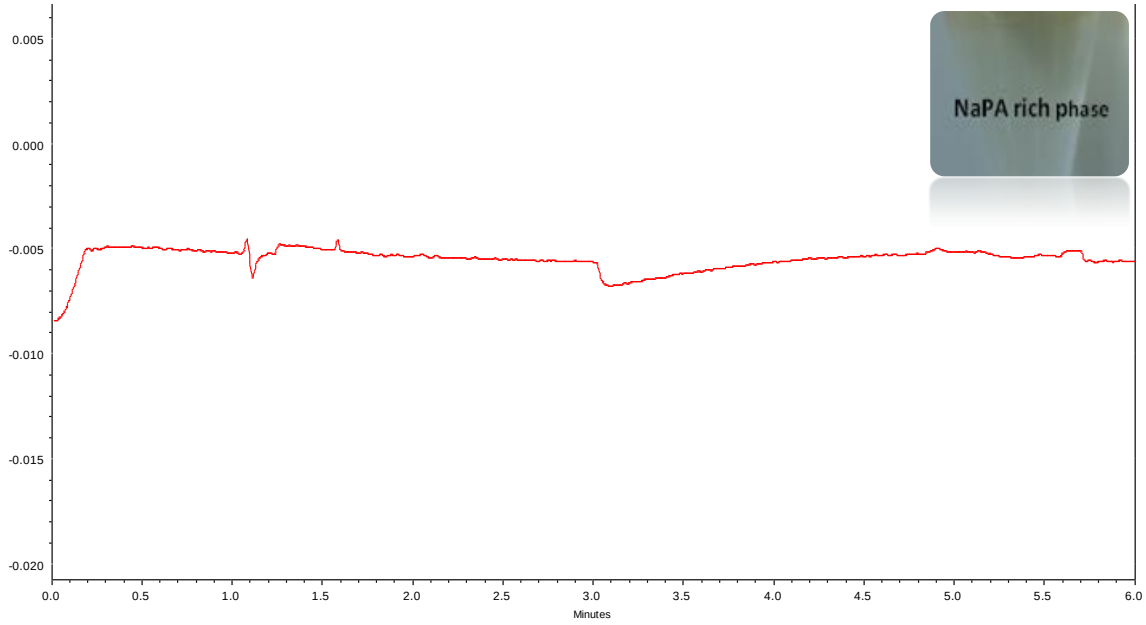

Figure 23. Electropherogram of NaPA 8000-rich phase of PEG 8000/NaPA 8000-based ABS with [C_2mim]Cl as electrolyte prepared using the *Ayahuasca* pre-treated sample. Conditions applied: MEKC buffer containing 20 mM sodium tetraborate, TBS (pH 9.40), 40 mM SDS, 10 % (v/v) of methanol. Capillary 20 cm to the detector and 50 µm i.d., Applied current: 70 µA, hydrodynamic injection 0.5 psi for 30 seconds, T = (293.1 ± 0.1) K, wavelength 336 nm.

2.4. Conclusions and future work

In summary, this work suggests that further studies should be performed in order to develop a proper IL-based ABS to concentrate benzoylecgonine from urine and hallucinogens from *Ayahuasca* preparations. Although the general picture here created indicates that IL-based ABS were not successfully applied as pre-treatment routes, slight visual evidences show that polymeric ABS may be a promising alternative. Moreover, a novel MEKC method was successfully developed and validated for the quantification of the two hallucinogens harmine and harmaline in mixture, showing more advantageous characteristics than previously reported CE methods.

The low levels of the target compounds (in ppm units for benzoylecgonine) are in fact the main drawback for the application of IL-based ABS. In this context, further conditions should be investigated, mostly by alternatively reducing the volume of each phase, in order to enhance the concentration step. Also, ILs can be used in SPME as extracting phases or even the use of ILs as hydrotropes to increase the drug solubility in aqueous solutions, thus overcoming the problems related to the LOD of the quantification techniques.

Chapter III

FPLC Purification of recombinant L-Asparaginase I from Saccharomyces cerevisiae expressed in Escherichia coli

Abstract

L-Asparaginase is known by its capacity to catalyse the hydrolysis of L-asparagine into L-aspartic acid and ammonia. The effective depletion of L-asparagine results in a cytotoxicity scenario for leukemic cells. This enzyme has been thus clinically acceptable as an anti-tumour agent for the effective treatment of acute lymphoblastic leukemia and lymphosarcoma. This biopharmaceutical is produced by fermentation processes and then, it needs to be correctly separated from the contaminants produced in the fermentation process. Here, the Affinity Chromatography is applied as a novel approach to purify (His)6-tagged recombinant L-Asparaginase I from *Saccharomyces cerevisiae* expressed in *Escherichia coli*. The Affinity Chromatography was performed on a Fast Protein Liquid Chromatography (FPLC) system using a Ni^{2+}-charged, 5 mL HiTrap IMAC FF. A linear gradient, running from 0 mM to 500 mM of imidazole at 5.0 $mL.min^{-1}$ was performed in order to identify the lowest imidazole concentration of the elution buffer that extracts the higher amount of L-Asparaginase I. This concentration range was further used in a step imidazole gradient. Two-step concentrations of the initial imidazole concentration (32.0 and 54.4 %) were applied. Polyacrylamide gel electrophoresis combined with silver staining and Nessler activity assay were used to confirm the presence of the purified L-Asparaginase I (≈ 45 kDa). In the gradient step, the eluted recombinant L-Asparaginase I showed a high specific activity of 110.1 ± 0.3 $IU.mg^{-1}$. Furthermore, a recovery of 81.03 ± 0.01 % was obtained meaning a purification factor of 17 times. In this sense, the FPLC process has undoubtedly proved to be an efficient tool for the purification of this enzyme.

3.1. State-of-art

Enzymes can be used to catalyze chemical reactions with high efficiency and specificity. Compared to conventional chemical processes, biocatalytic processes usually consume less energy, produce less waste and use less organic solvents. Moreover, the reactions are promoted at low or moderate temperatures, using preferably natural substrates, fermentation media or industrial wastes. The ability to evolve bioprocesses and bioproduction systems allows for major improvements in both economic and environmental performance. In this sense, enzyme production and purification by biotechnological industries permits a manufacturing facility to increase their profitability and capacity while maintaining or even reducing its environmental footprint. The major applications of enzymes are in food, pulp and paper, cosmetic and pharmaceutical industries. The medical and pharmaceutical application of enzymes covers a wide range of applications, including killing disease-causing microorganisms, prompting wound healing, and diagnosing certain diseases. In contrast to other industrial uses, where production is on a much larger scale; uses of medical and pharmaceutical enzyme applications generally require small quantities of highly purified enzymes. Enzymes and enzyme-generated products are administered to patients in very small doses; this is in order to avoid possible side effects[97,98].

The L-asparaginase, L-asparagine amidohydrolase [EC 3.5.1.1] is an enzyme, which catalyzes the hydrolysis of the amino group L-asparagine, forming aspartic acid and ammonia (Eq. 6):

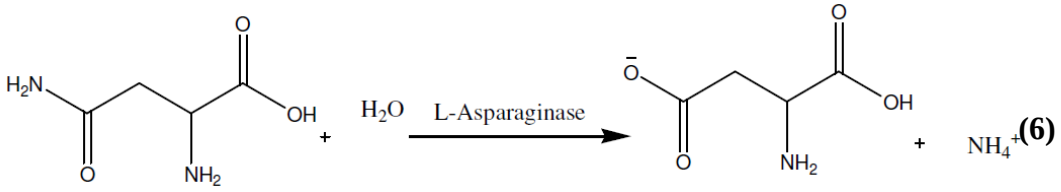

(6)

The discovery of this enzyme started by Kidd (1953)[99] remarkable observation, that Guinea pig serum had anti-tumor activity against several types of lymphoma in mice. The cause of this antileukemia activity was elucidated by Broome in 1963 proposed that the antileukaemia activity was attributed to the action of L-Asparaginase (L-ASNase)[100]. Nevertheless, only in 1967 the L-Asparaginase was isolated in quantities enough to be subjected to clinical trials towards to prove the anticancer activity[101]. Since then, the

interest in isolation and purification of L-ASNase has prominently improved, due to their pharmacological application.

L-ASNase was shown to be very useful in treating acute lymphocytic leukemia (ALL)[102–104], acute myeloid leukemia[105] and lymphomas[106]. Childhood acute lymphoblastic leukemia is a cancer of the blood and bone marrow[107,108]. In a healthy child, the bone marrow generates blood stem cells (immature cells) that become mature blood cells over time. A blood stem cell may become a myeloid stem cell or a lymphoid stem cell (Fig. 24). A myeloid stem cell becomes one of three types of mature blood cells: red blood cells that carry oxygen and other substances to all tissues of the body, platelets that form blood clots to stop bleeding and white blood cells that fight infection and disease. While a lymphoid stem cell becomes a lymphoblast cell and then one of three types of lymphocytes (white blood cells): lymphocytes that make antibodies to help fight infection; T lymphocytes that help B lymphocytes make the antibodies that help fight infection and natural killer cells that attack cancer cells and viruses.

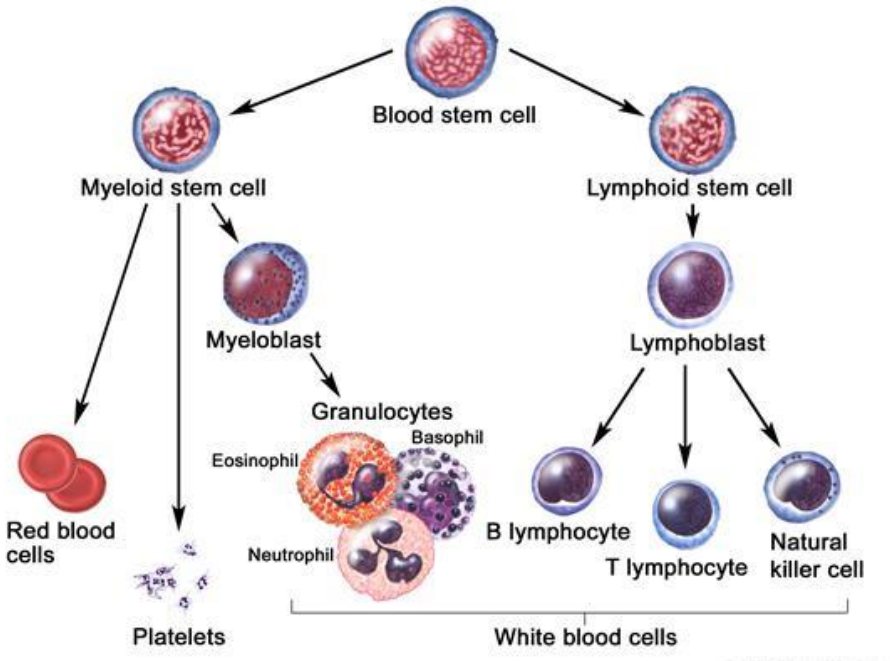

Figure 24. Overview of the normal human hematopoiesis[109]. Blood or Hematopoietic stem cells (HSCs) give rise to the myeloid (monocytes and macrophages, neutrophils, basophils, eosinophils, erythrocytes, megakaryocytes/platelets, dendritic cells), and lymphoid lineages (T-cells, B-cells, NK-cells)

In a child with ALL, too many stem cells become lymphoblasts, B lymphocytes, or T lymphocytes, leading towards to an overproduction of cancerous, immature white blood cells, known as lymphoblast. These cells are continuously multiplying, causing damage and death by inhibiting the production of normal cells, such as red and white blood cells

and platelets, in the bone marrow and by spreading (infiltrating) to other organs. The American Cancer Society's estimates in the United States for 2014, about 6020 new cases ALL (adults and children) and about 1440 deaths from ALL (adults and children), with much higher risk in children under 5 years old. Moreover, the average person's lifetime risk of getting ALL is less than 1 in 750, being this probability slightly higher in males than in females and also higher in whites than in African Americans[106–111].

Treatment options for newly diagnosed childhood ALL include the following three steps: remission induction, also known as chemotherapy, post-remission treatment, and maintenance therapy. In the first two phases L-ASNase is prescribed and administered intramuscularly or intravenously[103,104,106,112,113]. The lymphoblast cells require a large amount of asparagine (Asn) to enhance their rapid, malignant growth, thus are dependent the extracellular level of asparagine to perform their protein synthesis. Furthermore, lymphoblast cells are not able to induce synthesis of asparagine synthetase, which is an intracellular, inducible enzyme and responsible by the *de novo* synthesis of asparagine. In addition, ASNase has the critical role by the Asn hydrolysis (Eq. 6), resulting in drastic diminishing of asparagine level, leading the lymphoblast cells into metabolic collapse and consequently death. *In vitro* tests have shown that the asparagine level in blood becomes undetectable in some minutes, when the activity of L-ASNase is the order of 0.70 $IU.mL^{-1}$ [114]. The ability to reduce substantially the plasma level of asparagine and maintaining low for extended periods of time is the main feature responsible for the activity antineoplastic Asparaginase.

However, there are some factors limiting the use of L-ASNase as chemotherapy agent. One of the factors to be considered is the requirement of daily doses of parenteral injections from 10 to 200 IU/Kg/day for a period of time, which may last for 21 days. Another factor to be considered is the toxic side effects, *i.e.* hyperglycemia, fall serum albumin, lipoproteins and fibrinogen, increased liver fat and some dysfunctions mild brain[102,113,115–118]. The most important limiting factor is the development of hypersensitivity to treatment. This hypersensitivity reactions ranging from small allergy in the drug injection area, bronchospasm and even anaphylactic shock, suggesting that the patient should not be repeatedly subjected to the same treatments type of L-ASNase, occurs between 5 and 50% of treated patients.

Aiming to alleviate at least some of these problems, researches focus in protein structural modification, due through genetic engineering or gene enhancement; and moreover, in conjugation of L-ASNase with biopolymers (e.g. polyethylene glycol, dextran, albumin and heparin)[103,113,119–121]. With these modifications, other features were acquired, for example, enhanced resistance to inactivation by proteolytic enzymes, improved stereochemical specificity, decreasing their antigenic capacity, increase in affinity towards the target cell and extensive maintenance enzyme activity.

Nowadays, L-ASNase therapy is available in three preparations: two obtained from native forms, both bacterial and one preparation obtained from the *E. coli* enzyme conjugate with m-PEG [113]. *E. coli* and *Erwinia caratovora* are producing species of commercial L-Asparaginase from native forms (Elspar® from Merck and Erwinase® from Speywood, respectively). The two preparations exhibit similar mechanism of action and toxicity, differing in the pharmacokinetic properties [122,123].

In this study, the L-ASNase source was *Saccharomyces cerevisiae* X2180-1A. This microorganism synthesizes two forms of L-ASNase: L-ASNase I, an intracellular constitutive enzyme, and Asparaginase II, an external enzyme which is secreted in response to nitrogen starvation. These two enzymes are biochemically and genetically distinct. Sarquis et al[124], concluded that the usage of L-Asparaginase gene from an eukaryotic origin (yeast and filamentous fungi) can reduce the intensity of allergic reactions, due to post-translational modifications that occur in eukaryotic species, which are absent in prokaryotes beings. Therefore, it was studied the FPLC purification of L-ASNase I from *S. cerevisiae* cloned and expressed in *E.coli*. Fast protein liquid chromatography (FPLC), is a form of liquid chromatography that is mainly used to analyze or purify mixtures of proteins. As in other forms of chromatography, separation is possible because the different components of a mixture have different affinities for two materials, a moving fluid (the "mobile phase") and a porous solid (the stationary phase). In FPLC the mobile phase is an aqueous solution or "buffer". The buffer flow rate is controlled by a positive-displacement pump and it is normally kept constant, while the composition of the buffer can be varied by drawing fluids in different proportions from two or more external reservoirs. The stationary phase is a resin composed of beads, usually of cross-linked agarose, packed into a cylindrical glass or plastic column. FPLC resins are available in a wide range of bead sizes and surface ligands depending on the application. In this research,

we used immobilized metal ion affinity chromatography resin, which is ideal for purification of histidine-tagged recombinant proteins, due to the interaction between negatively charged histidines with nickel cations (Ni^{2+})[125].

3.2. Scopes

The development of techniques and methods for the separation and purification of proteins and other biomolecules has been paramount to many advances in the biotechnology industry[3,9,126]. The main challenge for the production of biomolecules of pharmacological interest is the large-scale purification, because the effective purification methods in the laboratory are usually not scalable and industrial purification methods require higher purity. There is a real need to find an alternative, rentable and eco-friendly way for L-ASNase purification. Therefore, our intention is to purify L-ASNase I with a low number of purifying steps, obtaining a pure enzyme with high yields and specific activity, in order to be scaled-up en route for a promissory commercial pharmaceutically application. The use of affinity chromatography performed on a Fast protein liquid chromatography (FPLC) system as downstream purifying technique is easily justified, since can be readily scaled from analysis of milligrams of mixtures in columns with a total volume of 5 mL or less to industrial production of kilograms of purified protein in columns with volumes of many liters. Moreover, in contrast to direct competitor, HPLC, the buffer pressure used is relatively low, typically less than 5 bar, but the flow rate is relatively high, typically 1-5 $mL.min^{-1}$, which is beneficial for protein purification.

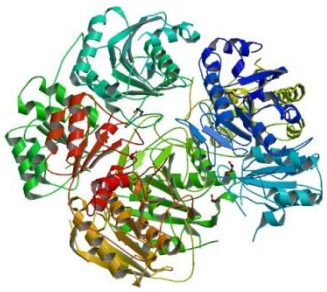

Figure 25. Schematic representation of the crystal L-asparaginase, resolution of 1.82 Å. (Extracted from Protein Data Bank, PDB code 2HIM).

3.3. Materials and Methods

3.3.1. Protein Expression

Initiators of ASNase I yeast (ASP1) were commissioned for the company Exxtend. For PCR amplification of this gene, was used the following protocol (Vf = 20 µL) : 1 µL of forward primer; 1 µL reverse primer ; 4 µl dNTPs (C = 1.25 mM); 0.4 µL $MgSO_4$ (C = 1 mM) ; 6 µL Platinum® Pfx DNA Polymerase (Invitrogen™); 10 µL Milli-Q water and 1 µl synthetic DNA of *S. cerevisiae* extracted with PureLink ® Pro 96 Genomic DNA Purification Kit (Invitrogen®) (ASP1 kit). Agarose gel to visualize the amplified samples : 0.8 % agarose (0.32 g) in 1x TAE buffer (40 mL). Addition 1.5 µL of ethidium bromide to mark nucleic acid and placed in a horizontal electrophoresis system connected to a voltage source of Bio Rad®.

Digestion of the vector pET15b and ASNase I: Restriction enzymes or endonucleases *Nde I* and *BamH I* were used (New England Biolabs, NEB), allowing the formation of cohesive ends in the DNA structures that will bind. The samples were incubated at 37 °C for 2 hours to VF = 100 mL: 1 µL high- fidelity *BamH I*; 2 µl NdeI ; 10 µL Buffer CutSmart 10X; 45 µL of ASNase I PCR product of yeast gene (ASP1) or bacterial vector pET15b and fully-filled with Milli-Q water. The purification of the digested samples is by cutting the agarose gel using the Illustra™ GFX™ PCR DNA and GEL BAND Purification Kit (GE®).

Insert the ASP1 gene into vector: 2 µL Buffer 5X T4 DNA ligase (Invitrogen) ; 2 µL pet15b vector digested and purified ; 5 µL insert (ASP1) digested and purified ; 1 µL T4 DNA ligase (1 $IU.\mu L^{-1}$). Afterwards, the mixture is incubated for 2 hours at room temperature (~ 25 ° C) or overnight at 16 ° C.

Bacterial Transformation: electrocompetent DH5α strain of *E. coli* bacteria stored in biofreezer -80 ° C were thawed and added to 1 µL of the ligation product; moved all content to electroporation cuvette which was placed in MicroPulser Electroporator (Bio Rad®) under the following conditions: 25 Ω conductance, 2.5 kV and 4.5-5.5 ms pulse. The transformation product was then resuspended in liquid LB medium (V = 1 mL) and incubated for 1 h at 37 °C under gentle agitation (70 rpm).

Centrifugation and all plating of the inoculum in Carbenicillin LB solid medium (C = 50 $\mu g.\mu L^{-1}$). Plates were incubated for 16 h at 37 °C. Then the selection of colonies in the

plate to be incubated in LB broth (~ 3 mL) and carbenicillin (~ 3 µL) in Falcon tubes was performed. Incubation was carried out at 37 ° C for 16 h.

Miniprep / alkaline lysis: Removal of plasmid + insert into bacteria by QIAprep Spin Miniprep Kit (Qiagen®) from 1.5 mL of culture medium, according to the manufacturer's instructions.

Heterologous expression of ASNases: *E. coli* BL21 (DE3) strain stored in refrigerator biofreezer -80 °C were thawed and added: 1 µL purified plasmid with the insert; moved all content to electroporation cuvette, which was placed in MicroPulser Electroporator (Bio Rad®) under the following conditions: 25 Ω conductance, 2.5 kV and 4.5-5.5 ms pulse. The transformation product was then resuspended in liquid LB medium (V = 1 mL) and incubated for 1 h at 37 °C under gentle agitation (70 rpm). The bacteria were grown in LB medium, supplemented with the appropriate antibiotics, at 37 °C until A_{600} = 0.6–0.7. When the bacteria are in log-phase, was added IPTG (Isopropylthio - β -D-galactoside) to induce transcription from the T7 promoter and consequently allow the production of ASNase I.

3.3.2. Cell lysis and sample pre-treatment

The sample pre-treatment was carried on by a chemical lysis procedure; herein cell pellets from genetically transformed *E. coli* were resuspended with BugBuster (10 mL *per* g cell), following the ensuing procedure: mixed gently for 20 minutes, in order to avoid foam formation; centrifuge at 16000 x *g* for 20 minutes at 4 °C; discard the pellet and the supernatant vacuum filter membrane (0.45 µm); add 20 mM final concentration imidazole to the filtered sample and finally apply sonication.

3.3.3. Ni^{2+}- affinity chromatography

Affinity chromatography was performed on FPLC™ System (ÄKTApurifier, GE Healthcare) using a $Ni2^{+}$-charged, 5 mL HiTrap IMAC FF column, ideal for purification of histidine-tagged recombinant proteins (Fig. 26).

A linear gradient, running from 0 mM to 500 mM of imidazole at 5.0 $mL.min^{-1}$ was performed in order to identify the lowest imidazole concentration of the elution buffer that extracts the higher amount of L-ASNase I. This concentration range was further used in a

step imidazole gradient, in which two-step concentrations of the initial imidazole concentration (32.0 and 54.4 %) were applied. The eluted fractions were collected with a fixed volume of 1.5 mL per fraction. The binding buffer (20 mM sodium phosphate buffer at pH = 8.0, 500 mM NaCl) and elution buffer (20 mM sodium phosphate buffer pH 8.0, 500mM NaCl, 500mM imidazole) were used in L-ASNase I purification.

Figure 26. (a) FPLC™ (System ÄKTApurifier) formed by Pump P-900, Monitor UV-900, Monitor UPC-900, Valve INV-907, Mixer M-925 and Valves SV-903, FV-923 (b) HiTrap™ 5 mL IMAC FF column

3.3.4. Nessler activity assay

The determination of enzymatic activity was performed by Nessler activity assay and expressed in $IU.mL^{-1}$ [127]. The samples are previously centrifuged 4000 x *g* for 20 min at 4°C, lysed and desalted with 20 mM Tris-HCl buffer at pH 8,6 (in order to remove imidazole). The sample volume of 0.1 mL is incubated at 37 °C for 30 min in 1 mL of Tris buffer (50 mM, pH 8.6) with 0.1 mL of L-asparagine (189 mM) and 0.9 mL of Milli-Q water, the reaction is stopped with the addiction of 0.1 mL trichloroacetic acid (TCA) 1.5 M. The tubes are shaken by inversion and centrifuged for 2 min to clarify. After staining step, 0.2 ml supernatant, 4.3 ml of Milli-Q water and 0.5 mL of Nessler reagent are mixed by inversion for 1 min and then measured in microplate reader at λ = 436 nm. To prepare the standard curve the amount of L-asparagine is replaced with (0.25, 0.50 and 1.0 mL) solution of ammonium sulfate (6 mM) and supplemented with Milli-Q water to 2.2 mL final volume. In order to remove the possible interferences, two blanks were made for each sample. Moreover, at least three samples of each enzymatic activity measure were prepared, decreasing the associated error of enzymatic activity quantification.

The enzymatic activity (EA) was calculated considering Eq. 7 and is expressed in IU.mL^{-1} enzyme:

$$EA = \frac{(\mu mole\ of\ NH_3\ liberated)}{t \times Ve} \quad \textbf{(7)}$$

where t corresponds to time of assay in minutes and Ve is the volume in mL of ASNase I used.

The specific activity (SA) was calculated following the Eq. 8 and is expressed in IU.mg^{-1} protein:

$$SA = \frac{EA}{[P]} \quad \textbf{(8)}$$

where EA corresponds to enzymatic activity in IU.mL^{-1} and [P] is the concentration of protein in mg of protein per mL of ASNase I used.

To evaluate the FPLC purification yield, two parameters were calculated, namely recovery and purification factor (PF), calculated by the following equations (Eq. 9 and 10)

$$Recovery\ \% = \frac{(EA)f}{(EA)i} \times 100 \quad \textbf{(9)}$$

$$PF = \frac{(SA)f}{(SA)i} \quad \textbf{(10)}$$

where (EA)f corresponds to enzymatic activity of the purified sample in IU/mL and (EA)I to enzymatic activity of the initial sample in IU/mL, meanwhile the (SA)f and (SA)i values are related to specific activity of the purified and the initial sample.

3.3.5. Protein quantification method

The absorbance assay, measuring the absorbance at λ = 280 nm, was used to estimate total protein concentration. This method is useful, due to the fact that the sample can be recovered and is the rapidest and most straightforward protein quantification method. A BSA calibration curve (bovine serum albumin, lyophilized powder, ≥ 96 wt%, Sigma®) was used to determine the protein concentration in the samples.

3.3.6. Polyacrylamide gel electrophoresis combined with silver staining

After FPLC purification, the samples are analyzed by SDS-PAGE technique. A sample volume of 20 μL is applied in polyacrylamide-gel, formed by 12% polyacrylamide-SDS (10 x 10.5 cm x 0.75 mm thick) under reducing conditions, according to the method of Laemmli[128]. The electrophoresis was performed at 120 V for approximately 1.5h using a vertical (Bio Rad®) system. Protein markers of different molar masses are bought in Bio Rad. The gels are silver stained for visualization of protein bands using the Silver Staining Kit (Amersham Pharmacia Biotech®) following the manufacturer's instructions.

3.4. Results and discussion

FPLC purification was performed in two different stages. In the first stage a linear gradient, running from 0 mM to 500 mM of imidazole at 5.0 $mL.min^{-1}$ was performed in order to identify the lowest imidazole concentration of the elution buffer that extracts the higher amount of L-ASNase I. By the analysis of the Fig. 27, there are two regions (fractions 14-18 and 20-31), in which a slightly increase in A_{280nm} was observed, this might indicate the elution of ASNase I from the nickel column. The washout unbound proteins, which not interact with the column, were eluted in fractions 4-5, where an intense peak of absorbance was obtained (this peak is not showed in Fig 27). Therefore, Nessler ASNase activity assay and electrophoresis were used to confirm the presence of the purified L-Asparaginase I (≈ 45 kDa). Through the Fig. 28 and the Table 2, we confirm that fractions 4-5 contain the proteins that have no interaction with nickel column and are immediately eluted, for this reason very low specific ASNase I activity were obtained (0.02 ± 0.00 $IU.mg^{-1}$). Moreover, the purified fractions 20-31 exhibit the highest specific activity (6.61 ± 0.08 $IU.mg^{-1}$) six times more than the fractions 14-1. Furthermore, by electrophoresis analysis, we can see that the bands from 22-31 are more intense, meaning that higher concentrations of ASNase I were purified in those fractions. Hence, it was determined to choose the imidazole concentration in the elution buffer that extracted fractions 23-30, respectively (32.0 and 54.4 % of the initial imidazole concentration in the elution buffer). This concentration range was further used in a step imidazole gradient, in which two-step concentrations of the initial imidazole concentration (32.0 and 54.4 %) were applied.

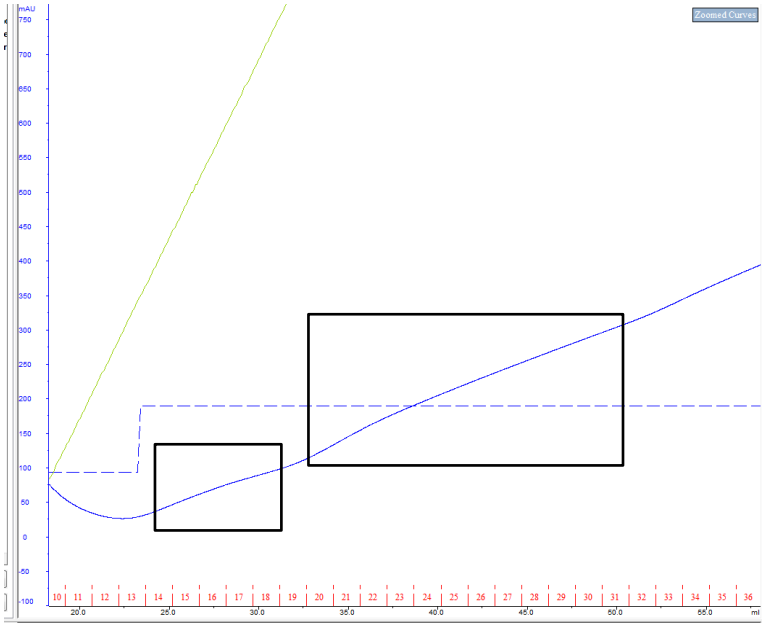

Figure 27. Linear gradient of imidazole used in FPLC purification, obtained from FPLC software. The blue line, corresponds to absorbance at 280 nm. The black boxes (fractions 14-18 and 20-31)

Table 2. FPLC purification with imidazole linear gradient (0 mM - 500 mM) at 5.0 mL.min^{-1}. Fractions eluted with ASNase I activity are shown, along with protein concentration, enzymatic activity and specific activity values.

Sample	*Protein Concentration (mg.mL^{-1})*	*Enzymatic activity (IU.mL^{-1})*	*Specific activity (IU.mg^{-1})*
Fractions 4-5	3.5442 ± 0.0002	0.0614 ± 0.0003	0.02 ± 0.00
Fractions 14-18	0.0536 ± 0.0107	0.0261 ± 0.0001	0.49 ± 0.00
Fractions 20-31	0.0170 ± 0.0021	0.1121 ± 0.0013	6.61 ± 0.08

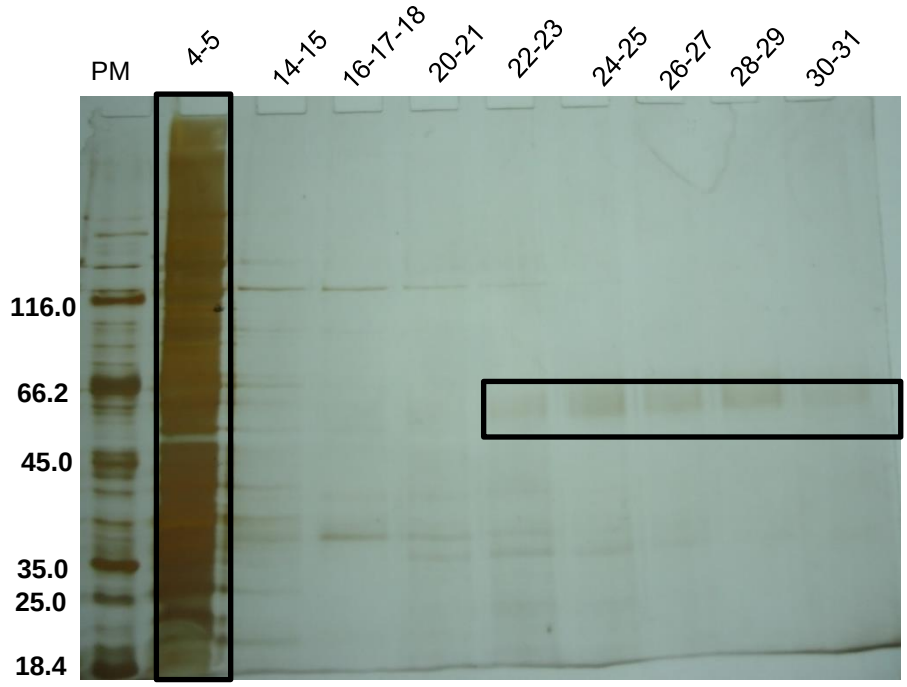

Figure 28. Polyacrylamide gel electrophoresis combined with silver staining, showing the purified samples from linear step FPLC purification. The black boxes highlight the wash-out unbound proteins (second lane) and histidine-tagged ASNase bands (~ 45.0 KDa). In the different lanes are represented the eluted fractions, PM refers to Protein Markers.

The second stage, the imidazole concentration in the elution buffer was optimized using a two-steps concentration. In the Table 3, it is evident that the elution fractions obtained in two-steps approach are much more purified than the ones obtained by linear gradient purification. Moreover, the eluted fractions 38-42 (total volume = 7.5 mL) were purified with higher specific ASNase I activity (110.06 ± 0.34 IU.mg^{-1}) and improved yields: a recovery of 81.03 ± 0.01 % was obtained, meaning a purification factor of 17 times. The electrophoresis (Fig. 29) is in good agreement with the previously results, confirming that the purified fractions have ASNase I in high concentrations.

Table 3. FPLC purification with two-step concentrations of the initial imidazole concentration (32.0 and 54.4 %) were applied.at 5.0 mL.min^{-1}. Fractions eluted with ASNase I activity are shown, along with protein concentration, enzymatic activity, specific activity, purification factor and recovery parameters.

Sample	*Protein Concentration (mg.mL^{-1})*	*Enzymatic activity (IU.mL^{-1})*	*Specific activity (IU.mg^{-1})*	*Purification factor*	*Recovery (%)*
Fermentation broth extract	0.3807 ± 0.0019	2.4898 ± 0.0014	6.52 ± 0.01	1.00	100.00
Fractions 28-32	0.0208 ± 0.0050	1.6022 ± 0.0081	79.87 ± 1.13	12.24	64.00
Fractions 33-37	0.0334 ± 0.0005	1.5103 ±0.0128	43.99 ± 0.43	6.75	60.66
Fractions 38-42	0.0185 ± 0.0025	2.0174 ±0.0052	110.06 ± 0.34	16.88	81.03

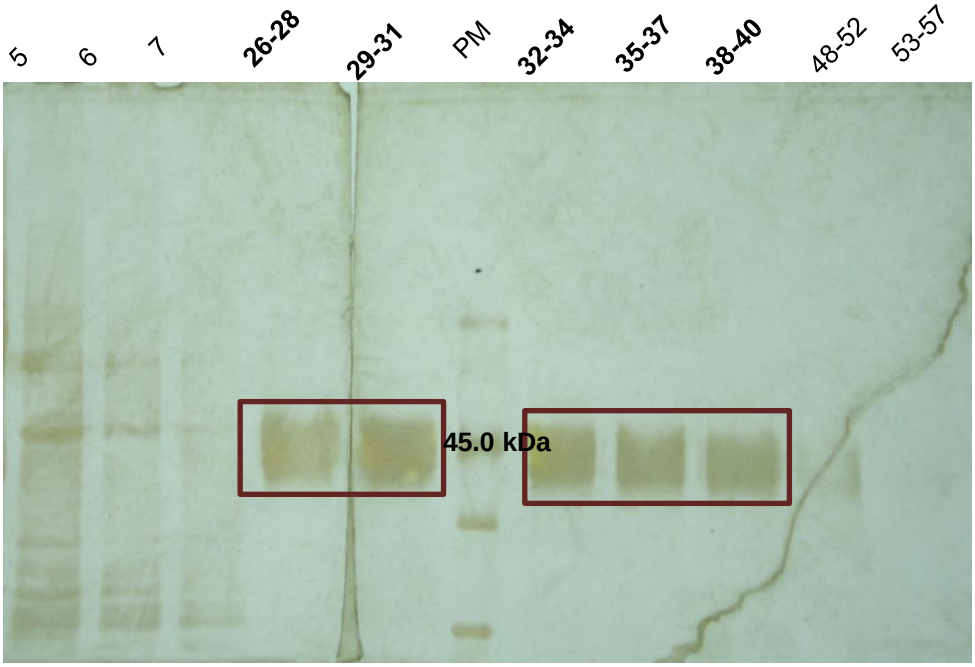

Figure 29. Polyacrylamide gel electrophoresis combined with silver staining, showing the purified samples from two-step FPLC purification. The brown box highlights the his-tagged ASNase bands (~ 45.0 KDa). In the different lanes are represented the eluted fractions, PM refers to Protein Markers.

3.5. Conclusions

In summary, the optimized two-steps FPLC purification method, allows a successful extraction and purification of L-ASNase I from *S cerevisiae* expressed in *E.coli*. This novel downstream method appears to be an eco-friendly and rentable alternative to purify L-ASNase I, which can be easily scaled up for industrial purposes. Upper yields and recovery were obtained; making FPLC an efficient tool for the purification of this particular enzyme.

3.6. Future work

Further studies in FPLC parameters, such as the fraction volume, pump pressure, initial volume injected, elution and binding buffer formulations should be achieved in order to even optimize more the purifying yields.

By the analysis of our results, the most purified fraction exhibit a lower specific activity (110 $IU.mg^{-1}$), when compared to the commercial ASNase formulations available in the market. Erwinaze® (Asparaginase from *Erwinia chrysanthemi*) and ELSPAR® (Asparaginase from recombinant *E. coli*) contains 225 $IU.mg^{-1}$, data displayed in Product Datasheet - Active Asparaginase full length protein ab73439. Through the decreasing of the fraction volume, higher specific activities will be reached, nearby the values of commercial L-ASNases.

General Conclusions

Aqueous biphasic systems and Fast Protein Liquid Chromatography were the two downstream techniques applied and studied in this research. When comparing the two techniques, it becomes notorious that in one hand ABS are high-throughput, low-resolution techniques and in the other hand FPLC is a high-resolution low-throughput technique. For that reason, ABS were used in purification of probe molecules with no contaminants presented and moreover used in toxicological field. Meanwhile, FPLC was applied in ASNase I purification, in order to obtain high yields and high purity levels to insure the product stability; since there are stringent quality requirements for products used for pharmaceutical purposes.

A novel downstream ABS technique was successfully developed, in which it's used low amounts of IL (0.1 wt%, for example) as an electrolyte that promote phase split of polymer components. Moreover, this new downstream technology proved to be advantageous to boost the extractive performance of different bio(molecules) including Cyt c and CA. Additionally, it is our intention to apply these types of ABS in the purification of added-value compounds from real matrices, such as fermentation media or marine raw materials.

Although, ABS were previously successful as an analytical tool for forensic toxicology field, *e.g.* bisphenol A purification from synthetic urine, their application is still scare, mainly because to the several obstacles that ABS faces. In this case ABS were not an advantageous single-step pre-treatment and extraction technique of both hallucinogens and cocaine biomarker from *Ayahuasca* and urine, respectively. This may be explained due to the following downstream challenges that this technique faces: toxins/drugs concentration is in minor levels (in the order $ng.mL^{-1}$) and both urine and *Ayahuasca* are two highly complex matrixes. For that reason, a higher-resolution downstream technique is needed in these cases.

The ASNase I purification from fermentation broth fulfilled the RIPP procedure. In which firstly, low-resolution techniques such as centrifugation, vacuum filtration and sonication were applied and only afterwards the high -resolution technique: FPLC.

References

(1) Shukla, A. A.; Hubbard, B.; Tressel, T.; Guhan, S.; Low, D. *Journal of Chromatography B: Analytical Technologies in the Biomedical and Life Sciences*, **2007**, *848*, 28–39.

(2) Ogez, J. R.; Hodgdon, J. C.; Beal, M. P.; Builder, S. E. *Biotechnol. Adv.* **1989**, *7*, 467–488.

(3) Carta, G.; Jungbauer, A. In *Protein Chromatography*; **2010**; pp. 1–55.

(4) Wieckhusen, D.; Beckmann, W. In *Crystallization: Basic Concepts and Industrial Applications*; **2013**; pp. 275–288.

(5) Green, D. P.; Gerber, A. S. *Polit. Anal.* **2002**, *10*, 394.

(6) Auramo, J.; Ala-risku, T. *International Journal of Logistics*, **2005**, *8*, 333–345.

(7) Cramer, S. M.; Holstein, M. A. *Curr. Opin. Chem. Eng.* **2011**, *1*, 27–37.

(8) Pierce. *Brochure*. **2010**, pp. 1–84.

(9) Kalyanpur, M. *Mol. Biotechnol.* **2002**, *22*, 87–98.

(10) Mazzola, P. G.; Lopes, A. M.; Hasmann, F. A.; Jozala, A. F.; Penna, T. C. V; Magalhaes, P. O.; Rangel-Yagui, C. O.; Pessoa, A. *Journal of Chemical Technology and Biotechnology*, **2008**, *83*, 143–157.

(11) Albertsson, P.A. *Nature* **1958**, *182*, 709–711.

(12) Martínez-Aragón, M.; Burghoff, S.; Goetheer, E. L. V; de Haan, A. B. *Sep. Purif. Technol.* **2009**, *65*, 65–72.

(13) Asenjo, J. A.; Andrews, B. A.. *Journal of Chromatography A*, **2011**, *1218*, 8826–8835.

(14) Johansson, H.-O.; Ishii, M.; Minaguti, M.; Feitosa, E.; Penna, T. C. V.; Pessoa, A. *Separation and Purification Technology*, **2008**, *62*, 166–174.

(15) Johansson, H.-O.; Magaldi, F. M.; Feitosa, E.; Pessoa, A. *J. Chromatogr. A* **2008**, *1178*, 145–153.

(16) Deive, F. J.; Rodríguez, A.; Pereiro, A. B.; Araújo, J. M. M.; Longo, M. A.; Coelho, M. A. Z.; Lopes, J. N. C.; Esperança, J. M. S. S.; Rebelo, L. P. N.; Marrucho, I. M.. *Green Chemistry*, **2011**, *13*, 390.

(17) Rito-Palomares, M.; Negrete, a; Miranda, L.; Flores, C.; Galindo, E.; Serrano-Carreón, L. *Enzyme Microb. Technol.* **2001**, *28*, 625–631.

(18) Albertsson, P. A. *Adv. Protein Chem.* **1970**, *24*, 309–341.

(19) Rosa, P. A. J.; Azevedo, A. M.; Sommerfeld, S.; Bäcker, W.; Aires-Barros, M. R. *Biotechnology Advances*, **2011**, *29*, 559–567.

(20) Hirata, D. B.; Badino, A. C. J.; Hokka, C. O. In *2nd Mercosur Congress on Chemical Engineering and 4th Mercosur Congress on Process Systems Engineering*; **2005**; pp. 1–6.

(21) Haga, R. B.; Santos-Ebinuma, V. C.; De Siqueira Cardoso Silva, M.; Pessoa, A.; Rangel-Yagui, C. O. *Sep. Purif. Technol.* **2013**, *103*, 273–278.

(22) Viana Marques, D. A.; Pessoa-Júnior, A.; Lima-Filho, J. L.; Converti, A.; Perego, P.; Porto, A. L. F. *Biotechnol. Prog.* **2011**, *27*, 95–103.

(23) Da Silva, L. M.; Meirelles, A. A. *Carbohydr. Polym.* **2000**, *42*, 273–278.

(24) Da Silva, L. H. M.; Meirelles, A. J. A. *Carbohydr. Polym.* **2001**, *46*, 267–274.

(25) Azevedo, A. M.; Rosa, P. A. J.; Ferreira, I. F.; Aires-Barros, M. R. *J. Biotechnol.* **2007**, *132*, 209–217.

(26) Zafarani-Moattar, M. T.; Sadeghi, R. *J. Chem. Eng. Data* **2005**, *50*, 947–950.

(27) Bridges, N. J.; Gutowski, K. E.; Rogers, R. D. *Green Chemistry*, **2007**, *9*, 177.

(28) Freire, M. G.; Cláudio, A. F. M.; Araújo, J. M. M.; Coutinho, J. A. P.; Marrucho, I. M.; Lopes, J. N. C.; Rebelo, L. P. N. *Chemical Society Reviews*, **2012**, *41*, 4966.

(29) Passos, H.; Ferreira, A. R.; Cláudio, A. F. M.; Coutinho, J. A. P.; Freire, M. G. *Biochem. Eng. J.* **2012**, *67*, 68–76.

(30) Sintra, T. E.; Cruz, R.; Ventura, S. P. M.; Coutinho, J. A. P. *Journal of Chemical Thermodynamics*, **2013**, 10, 10-16.

(31) Johansson, G.; Reczey, K. *J. Chromatogr. B Biomed. Appl.* **1998**, *711*, 161–172.

(32) Johansson, H.-O.; Feitosa, E.; Junior, A. P. *Polymers*, **2011**, *3*, 587–601.

(33) Gupta, V.; Nath, S.; Chand, S. *Polymer*, **2002**, *43*, 3387–3390.

(34) Saravanan, S.; Rao, J. R.; Nair, B. U.; Ramasami, T. *Process Biochemistry*, **2008**, *43*, 905–911.

(35) Pereira, J. F. B.; Rebelo, L. P. N.; Rogers, R. D.; Coutinho, J. a P.; Freire, M. G. *Phys. Chem. Chem. Phys.* **2013**, *15*, 19580–19583.

(36) Pereira, J. F. B.; Ventura, S. P. M.; E Silva, F. A.; Shahriari, S.; Freire, M. G.; Coutinho, J. A. P. *Sep. Purif. Technol.* **2013**, *113*, 83–89.

(37) Jiang, Y.; Xia, H.; Yu, J.; Guo, C.; Liu, H. *Chem. Eng. J.* **2009**, *147*, 22–26.

(38) De Souza, R. L.; Campos, V. C.; Ventura, S. P. M.; Soares, C. M. F.; Coutinho, J. A. P.; Lima, Á. S. *Fluid Phase Equilib.* **2014**, *375*, 30–36.

(39) Almeida, M. R.; Passos, H.; Pereira, M. M.; Lima, Á.S.; Coutinho, J. A. P.; Freire, M. G. *Sep. Purif. Technol.* **2014**, *128*, 1–10.

(40) Pereira, J. F. B.; Lima, Á. S.; Freire, M. G.; Coutinho, J. A. P. *Green Chemistry*, **2010**, *12*, 1661.

(41) Galiński, M.; Lewandowski, A.; Stepniak, I. *Electrochimica Acta*, **2006**, *51*, 5567–5580.

(42) Freemantle, M. *Chem. Eng. News Arch.* **1998**, *76*, 32–37.

(43) Bushnell, G. W.; Louie, G. V; Brayer, G. D. *J. Mol. Biol.* **1990**, *214*, 585–595.

(44) Ali, S. A. M. and S. N. *Medicinal Chemistry*, **2013**, *3*, 241-246.

(45) Ventura, S. P. M.; Neves, C. M. S. S.; Freire, M. G.; Marrucho, I. M.; Oliveira, J.; Coutinho, J. A. P. *J. Phys. Chem. B* **2009**, *113*, 9304–9310.

(46) Merchuk, J. C.; Andrews, B. A.; Asenjo, J. A. *J. Chromatogr. B. Biomed. Sci. Appl.* **1998**, *711*, 285–293.

(47) E Silva, F. A.; Sintra, T.; Ventura, S. P. M.; Coutinho, J. A. P. *Sep. Purif. Technol.* **2014**, *122*, 315–322.

(48) Cláudio, A. F. M.; Swift, L.; Hallett, J. P.; Welton, T.; Coutinho, J. A. P.; Freire, M. G. *Phys. Chem. Chem. Phys.* **2014**, *16*, 6593–6601.

(49) Limaye, P. B.; Shankar, K.; Apte, U. M.; Vaidya, V. S. *International Journal of Toxicology*, **2001**, *20*, 333–335.

(50) Stout, P. R. In *Information Resources in Toxicology*; **2009**; pp. 293–296.

(51) Kabir, A.; Holness, H.; Furton, K. G.; Almirall, J. R. *Trends in Analytical Chemistry*, **2013**, *45*, 264–279.

(52) Kole, P. L.; Venkatesh, G.; Kotecha, J.; Sheshala, R. *Biomedical Chromatography*, **2011**, *25*, 199–217.

(53) Gutowski, K. E.; Broker, G. A.; Willauer, H. D.; Huddleston, J. G.; Swatloski, R. P.; Holbrey, J. D.; Rogers, R. D. *J. Am. Chem. Soc.* **2003**, *125*, 6632–6633.

(54) Ventura, S. P. M.; Santos-Ebinuma, V. C.; Pereira, J. F. B.; Teixeira, M. F. S.; Pessoa, A.; Coutinho, J. A. P. *J. Ind. Microbiol. Biotechnol.* **2013**, *40*, 507–516.

(55) Ventura, S. P. M.; de Barros, R. L. F.; de Pinho Barbosa, J. M.; Soares, C. M. F.; Lima, Á. S.; Coutinho, J. A. P. *Green Chemistry*, **2012**, *14*, 734.

(56) Freire, M. G.; Teles, A. R. R.; Canongia Lopes, J. N.; Rebelo, L. P. N.; Marrucho, I. M.; Coutinho, J. A. P.. *Separation Science and Technology*, **2012,** *47*, 284–291.

(57) Passos, H.; Sousa, A. C. A.; Pastorinho, M. R.; Nogueira, A. J. A.; Rebelo, L. P. N.; Coutinho, J. A. P.; Freire, M. G. *Analytical Methods*, **2012**, *4*, 2664.

(58) Li, S.; He, C.; Liu, H.; Li, K.; Liu, F. *J. Chromatogr. B Anal. Technol. Biomed. Life Sci.* **2005**, *826*, 58–62.

(59) Sun, L.; Lau, C. E. *Drug Metab. Dispos.* **2001**, *29*, 1183–1189.

(60) Yao, D.; Shi, X.; Wang, L.; Gosnell, B. a; Chen, C. *Drug Metab. Dispos.* **2013**, *41*, 79–88.

(61) Goeders, N. E. *J. Pharmacol. Exp. Ther.* **2002**, *301*, 785–789.

(62) McGinty, J. F.; Whitfield, T. W.; Berglind, W. J. *Brain Res.* **2010**, *1314*, 183–193.

(63) Zhang, J. Y.; Foltz, R. L. *J. Anal. Toxicol.* **1990**, *14* , 201–205.

(64) Billings, K. E. *Illinois Wesley. Univ. Digit. Commons* **2003**.

(65) Hamilton, H. E.; Wallace, J. E.; Shimek, E. L.; Land, P.; Harris, S. C.; Christenson, J. G. *J. Forensic Sci.* **1977**, *22*, 697–707.

(66) Pereira De Toledo, F. C.; Yonamine, M.; De Moraes Moreau, R. L.; Silva, O. A. *J. Chromatogr. B Anal. Technol. Biomed. Life Sci.* **2003**, *798*, 361–365.

(67) Romolo, F. S.; Rotolo, M. C.; Palmi, I.; Pacifici, R.; Lopez, A. *Forensic Sci. Int.* **2003**, *138*, 17–26.

(68) Moore, C.; Coulter, C.; Crompton, K. *J. Chromatogr. B Anal. Technol. Biomed. Life Sci.* **2007**, *859*, 208–212.

(69) Favretto, D.; Pascali, J. P.; Tagliaro, F. *J. Chromatogr. A* **2013**, *1287*, 84–95.

(70) Huang, Y.-S.; Liu, J.-T.; Lin, L.-C.; Lin, C.-H. *Electrophoresis* **2003**, *24*, 1097–1104.

(71) Antonilli, L.; Suriano, C.; Grassi, M. C.; Nencini, P. *J. Chromatogr. B. Biomed. Sci. Appl.* **2001**, *751*, 19–27.

(72) Hall, B. J.; Parikh, A. R.; Brodbelt, J. S. *J. Forensic Sci.* **1999**, *44*, 527–534.

(73) Schramm, W.; Craig, P. A.; Smith, R. H.; Berger, G. E. *Clin. Chem.* **1993**, *39*, 481–487.

(74) Jones, A. W.; Holmgren, A.; Kugelberg, F. C. *Forensic Sci. Int.* **2008**, *177*, 133–139.

(75) Clauwaert, K. M.; Van Bocxlaer, J. F.; Lambert, W. E.; De Leenheer, A. P. *Anal. Chem.* **1996**, *68*, 3021–3028.

(76) Corburt, M. R.; Koves, E. M. *J. Forensic Sci.* **1994**, *39*, 136–149.

(77) Musshoff, F.; Madea, B. *Forensic Sci. Int.* **2010**, *200*, 67–72.

(78) Virag, L.; Jamdar, S.; Chao, C. R.; Morishima, H. O. *J. Chromatogr. B Biomed. Appl.* **1994**, *658*, 135–141.

(79) Riba, J.; Bouso, J. C. J. C. In *The Ethnopharmacology of Ayahuasca*; **2011**; Vol. 661, pp. 56–63.

(80) Riba, J.; Valle, M.; Urbano, G.; Yritia, M.; Morte, A.; Barbanoj, M. J. *J Pharmacol Exp.*; **2003**; Vol. 306, pp. 73–83.

(81) McKenna, D. J. In *Pharmacology and Therapeutics*; **2004**; Vol. 102, pp. 111–129.

(82) Pires, A. P. S.; De Oliveira, C. D. R.; Moura, S.; Dorr, F. A.; Silva, W. A. E.; Yonamine, M. *Phytochem. Anal.* **2009**, *20*, 149–153.

(83) Brierley, D. I.; Davidson, C. *Progress in Neuro-Psychopharmacology and Biological Psychiatry*, **2012**, *39*, 263–272.

(84) McKenna, D. J.; Callaway, J. C.; Grob, C. S. *Heffer Rev. Psychedelic Res.* **1998**, *1*, 65–76.

(85) Riba, J.; Rodríguez-Fornells, A.; Urbano, G.; Morte, A.; Antonijoan, R.; Montero, M.; Callaway, J. C.; Barbanoj, M. J. *Psychopharmacology (Berl).* **2001**, *154*, 85–95.

(86) Levêque, D.; Gailion-Renault, C.; Monteil, H.; Jehl, F. *J. Chromatogr. B. Biomed. Sci. Appl.* **1997**, *697*, 67–75.

(87) Weinberger, R.; Lurie, I. S. *Anal. Chem.* **1991**, *63*, 823–827.

(88) Kuroda, Y.; Shibukawa, A.; Nakagawa, T. *Yakugaku Zasshi* **2003**, *123*, 781–788.

(89) Fang, C.; Chung, Y.-L.; Liu, J.-T.; Lin, C.-H. *Forensic Sci. Int.* **2002**, *125*, 142–148.

(90) Anastos, N.; Barnett, N. W.; Lewis, S. W. *Talanta* **2005**, *67*, 269–279.

(91) Manetto, G.; Crivellente, F.; Tagliaro, F. *Ther. Drug Monit.* **2000**, *22*, 84–88.

(92) Tagliaro, F.; Bortolotti, F.; Pascali, J. P. *Anal. Bioanal. Chem.* **2007**, *388*, 1359–1364.

(93) Rittgen, J.; Pütz, M.; Pyell, U. *Electrophoresis* **2008**, *29*, 2094–2100.

(94) Webb, R.; Doble, P.; Dawson, M. *Electrophoresis* **2007**, *28*, 3553–3565.

(95) Ventura, S. P. M.; Sousa, S. G.; Serafim, L. S.; Lima, A. S.; Freire, M. G.; Coutinho, J. A. P. *J. Chem. Eng. Data* **2012**, *57*, 507–512.

(96) Cheng, J.; Mitchelson, K. R. *J. Chromatogr. A* **1997**, *761*, 297–305.

(97) Wang, M.; Si, T.; Zhao, H. *Bioresour. Technol.* **2012**, *115*, 117–125.

(98) Robertson, D. E.; Steer, B. A. *Current Opinion in Chemical Biology*, **2004**, *8*, 141–149.

(99) Kidd, J. G. *J. Exp. Med.* **1953**, *98*, 565–582.

(100) Broome, J. D. *J. Exp. Med.* **1968**, *127*, 1055–1072.

(101) Wade, H. E.; Robinson, H. K.; Phillips, B. W. *J. Gen. Microbiol.* **1971**, *69*, 299–312.

(102) Rizzari, C.; Conter, V.; Starý, J.; Colombini, A.; Moericke, A.; Schrappe, M. *Curr. Opin. Oncol.* **2013**, *25 Suppl 1*, S1–9.

(103) Pieters, R.; Hunger, S. P.; Boos, J.; Rizzari, C.; Silverman, L.; Baruchel, A.; Goekbuget, N.; Schrappe, M.; Pui, C.-H. *Cancer* **2011**, *117*, 238–249.

(104) Piatkowska-Jakubas, B.; Krawczyk-Kuliś, M.; Giebel, S.; Adamczyk-Cioch, M.; Czyz, A.; Lech Marańda, E.; Paluszewska, M.; Pałynyczko, G.; Piszcz, J.; Hołowiecki, J. *Pol. Arch. Med. Wewn.* **2008**, *118*, 664–669.

(105) Takahashi, H.; Koh, K.; Kato, M.; Kishimoto, H.; Oguma, E.; Hanada, R. *Int. J. Hematol.* **2012**, *96*, 136–140.

(106) Beard, M. E.; Crowther, D.; Galton, D. A.; Guyer, R. J.; Fairley, G. H.; Kay, H. E.; Knapton, P. J.; Malpas, J. S.; Scott, R. B. *Br. Med. J.* **1970**, *1*, 191–195.

(107) Pui, C.-H.; Robison, L. L.; Look, A. T. *Lancet* **2008**, *371*, 1030–1043.

(108) Pui, C.-H.; Relling, M. V; Downing, J. R. *N. Engl. J. Med.* **2004**, *350*, 1535–1548.

(109) Inaba, H.; Greaves, M.; Mullighan, C. G. *Lancet* **2013**, *381*, 1943–1955.

(110) Onciu, M. *Hematology/Oncology Clinics of North America*, **2009**, *23*, 655–674.

(111) Pui, C.-H.; Mullighan, C. G.; Evans, W. E.; Relling, M. V. *Blood* **2012**, *120*, 1165–1174.

(112) Ortega, J. A.; Nesbit, M. E.; Donaldson, M. H.; Hittle, R. E.; Weiner, J.; Karon, M.; Hammond, D. *Cancer Res.* **1977**, *37*, 535–540.

(113) Narta, U. K.; Kanwar, S. S.; Azmi, W. *Critical Reviews in Oncology/Hematology*, **2007**, *61*, 208–221.

(114) Story, M. D.; Voehringer, D. W.; Stephens, L. C.; Meyn, R. E. *Cancer Chemother. Pharmacol.* **1993**, *32*, 129–133.

(115) Billett, A. L.; Carls, A.; Gelber, R. D.; Sallan, S. E. *Cancer* **1992**, *70*, 201–206.

(116) Raja, R. A.; Schmiegelow, K.; Frandsen, T. L. *British Journal of Haematology*, 2012, *159*, 18–27.

(117) Knoderer, H. M.; Robarge, J.; Flockhart, D. A. *Pediatr. Blood Cancer* **2007**, *49*, 634–639.

(118) Schleis, S. E.; Rizzo, S. A.; Phillips, J. C.; LeBlanc, A. K. *Can. Vet. J.* **2011**, *52*, 1009–1012.

(119) Van den Berg, H. *Leuk. Lymphoma* **2011**, *52*, 168–178.

(120) Keating, M. J.; Holmes, R.; Lerner, S.; Ho, D. H. *Leuk. Lymphoma* **1993**, *10 Suppl*, 153–157.

(121) Fu, C. H.; Sakamoto, K. M. *Expert Opin. Pharmacother.* **2007**, *8*, 1977–1984.

(122) Guo, Q.-L.; Wu, M.-S.; Chen, Z. *Acta Pharmacol. Sin.* **2002**, *23*, 946–951.

(123) Soares, A. L.; Guimarães, G. M.; Polakiewicz, B.; Pitombo, R. N. D. M.; Abrahão-Neto, J. *Int. J. Pharm.* **2002**, *237*, 163–170.

(124) Sarquis, M. I. de M.; Oliveira, E. M. M.; Santos, A. S.; Costa, G. L. da. *Mem. Inst. Oswaldo Cruz* **2004**, *99*, 489–492.

(125) Amersham. *Manual*. **2000**, pp. 1–65.

(126) Ghasem D., N. In *Biochemical Engineering and Biotechnology*; **2007**, pp. 390–415.

(127) Imada, A.; Igarasi, S.; Nakahama K. *Microbiology* **1973**, *76*, 85–89.

(128) Laemmli, U. K. *Nature* **1970**, *227*, 680–685.

Acknowledgements

The authors are grateful for financial support from FEDER funds through the program COMPETE and by national fund through the Portuguese Foundation for Science and Technology (FCT) under the scope of the project Pest-C/CTM/LA0011/2013. The authors also thank financial support through the post-doctoral grant SFRH/BPD/79263/2011 of S.P.M. Ventura, Santander Scholarship granted to João H. Santos. The authors also thank the financial support from FAPESP through the project FAPESP 2012/12022-6. This project was also afford by Coordenação de Aperfeiçoamento de Pessoal de Nível Superior (CAPES) and Conselho Nacional de Desenvolvimento Científico e Tecnológico (CNPq) from Brazil.